

A high-resolution perspective on MIS 5c-d lithic assemblages from Klasies River main site Cave 1

Mareike J. Brenner^{a,*}, Sarah Wurz^{a,b}

^a Archaeology Department, School of Geography, Archaeology and Environmental Studies, University of the Witwatersrand, Johannesburg, Gauteng, South Africa

^b SFF Centre for Early Sapiens Behaviour (SapienCE), University of Bergen, Post Box 7805, 5020, Norway

ARTICLE INFO

Keywords:

MIS 5 lithic technology
Middle Stone Age
Marine isotope stage 5c-d

ABSTRACT

Klasies River contains an extensive MIS 5 MSA sequence, mostly from what has been described as the MSA II, MSA 2a or the Mossel Bay techno-complex. The current Witness Baulk excavations undertaken between 2015 and 2016 allows for a renewed and detailed investigation of the variability of the lithic technology from the lowermost part of the MSA II. This assemblage is equivalent to Deacon's SASL sub-member and Layers 17a and b of Singer and Wymer. Two phases are recognized: An MIS 5c phase in layer SMONE (Singer & Wymer layer 17a) and an MIS 5d phase in layers BOS One and BOS Two (Singer & Wymer layer 17 b). The two phases are characterized by commonalities such as a focus on quartzite utilisation, the presence of a main unidirectional reduction system, similar end products which comprise of points, blades and flakes and a low amount of formal tools. However, this high-resolution investigation of the layers reveals temporal variability. In the Shell Midden ONE (SMONE) layer cores and products are relatively lighter and small debitage is more frequent. There are more flake end products and compared to the lower layer, there are fewer tool types. In the Black Occupational Soil (BOS) layer points and blades are more numerous, products are heavier, core types are more variable, and a higher frequency and variety of tool types occur. Such detailed differences within the MIS 5 assemblages from Klasies River, not described before, shows that the MSA II is not a homogeneous entity, and that subtle patterning occurs that may link to different technological strategies. Compared to other MIS 5 sites on the southern Cape, namely Blombos Cave, Pinnacle Point and Cape St. Blaize, a common pattern in place provisioning is seen, although the technology shows differences between the sites. This study indicates the value of more detailed studies of MIS 5 assemblages as a tool to understand variability from a more refined perspective.

1. Introduction

1.1. Research history and background

Klasies River main site (KRM) has been recognized for its archaeological value at least since the 1950's when the site was brought to the attention of the South African Archaeological Society (Singer and Wymer, 1982, p. 7). Since then, the site has been declared a national monument or Grade 1 site (Deacon, 1995; Wurz et al., 2018). KRM is a unit of five closely located caves and shelters including Caves 1, 1A, 1B, 1C and 2. The site took its name from the near-by river Klasies, which disembogues 0.5 km west of main site. Main site is located on the Tsitsikamma coast of the Southern Cape, an area that receives rainfall throughout the year (Compton, 2011, p. 509; Carr et al., 2016, p. 28). The current vegetation at the Klasies River sites and its immediate environment are characterized by a complex mosaic of thicket, forest

and coastal vegetation with some fynbos elements (Cowling, 1984; van Wijk et al., 2017). Natural springs occur plenty-full uphill of the caves (Singer and Wymer, 1982, p. 8). The caves and overhangs are situated in a cliff topped by a calcarenite dune that is the source of lime-rich waters that led to the formation of flowstone, stalagmites and stalactites. This environment is also favourable for the preservation of bones, which was one of the reasons Singer chose to investigate the Klasies River Caves. Singer (Singer and Wymer, 1982, p. 8) was in search of an undisturbed Pleistocene site which could yield bone preservation, in order to contribute research to his main interest, the development of human physical and cultural evolution in South Africa. Excavations started at the end of 1966 under the direction of Singer's colleague Wymer, who undertook two field seasons at KRM between 1966 and 1968 (Singer and Wymer, 1982, p. 7). They excavated vast amounts of material from the caves including parts of an extensive sequence of > 20 m of deposit from the Middle Stone Age (MSA). This

* Corresponding author.

E-mail address: mareike.j.brenner@gmail.com (M.J. Brenner).

revealed insights into the MSA culture-stratigraphic succession which displays distinctly different phases through time.

Most of Cave 1 was excavated in trenches or cuttings down to the bedrock (Singer and Wymer, 1982, Fig. 2.1). Wymer (Singer and Wymer, 1982, p. 8) left a ca. 3 m high Witness Baulk in the centre stretching for > 12 m from the entrance to the back of the cave (Fig. 2). Various areas of main site, including the Witness Baulk, were investigated over multiple seasons by Deacon (Deacon and Geleijnse, 1988; Deacon, 1995), who undertook excavations from 1984 to 1995 (Fig. 2). The Deacon excavations of the MSA deposits of the Witness Baulk did not reach bedrock and ended within the lower phases of the MSA II, a techno-complex dating to MIS 5. Excavations resumed in 2015 by Wurz targeting the remaining lowermost deposits within the Witness Baulk (Wurz et al., 2018).

KRM plays a significant role in understanding the evolution of anatomically modern humans during Marine Isotope Stage (MIS) 5 (Grine et al., 2017). The presence of anatomically modern humans in South Africa during MIS 5 is reflected in occupational deposits of a number of MSA sites, including Blombos Cave, Cape St Blaize (Goodwin and Malan, 1935; Thompson and Marean, 2008), Die Kelders (Avery et al., 1997), Diepkloof Rock Shelter (Porraz et al., 2013a, 2013b), Hoedjiespunt (Will et al., 2013), Klasies River main site (Singer and Wymer, 1982; Deacon, 1995; Wurz, 2002), Pinnacle Point (Thompson et al., 2010; Brown, 2011) and possibly Blind River (Wang et al., 2008), Elands Bay Cave (Schmid et al., 2016) and Ysterfontein 1 (Avery et al., 2008; Wurz, 2012) on the western and southern coast, as well as sites from the interior such as Border Cave (Backwell et al., 2018), Bushman Rockshelter (Porraz et al., 2018), Florisbad (Kuman et al., 1999), Putslaagte 8 (Mackay et al., 2015) and Sibudu (Rots et al., 2017) (Fig. 1). Despite the significant human footprint during this time period, human fossils dating to MIS 5 are quite rare and occur only at Blind River, Klasies River and Pinnacle Point (Dusseldorp et al., 2013; Grine et al., 2017). At Pinnacle Point two fossils and at KRM > 50 fossils are directly associated with MIS 5 lithic technology. At KRM, five human remains, including three skull fragments, one mandible and one ulna excavated by Wymer are from the SASL member from other parts of the

Cave 1/1A (Grine et al., 2017, p. 46). The lithics from the associated SASL member within the Witness Baulk are discussed in this paper (see Figs. 2 and 3).

1.2. MIS 5 lithic technology

MIS 5 lithic technology in South Africa, in general, is characterized by the use of local raw materials, a low amount of formal tools with denticulates, notches and scrapers as the main tool types (Douze et al., 2015; Mackay, 2016). However, there are exceptions in the formal tool component, in that some other tool types occur frequently but only in specific sites, for example end scrapers at Bushman Rock Shelter and serrated pieces at Sibudu (Rots et al., 2017). It is also worth mentioning that some Pre-Still Bay assemblages show a much higher frequency of tools, as is seen at Diepkloof (Porraz et al., 2013b). MIS 5 assemblages thus cannot be adequately described with typology as universal *fossils directeurs* for this time period does not occur. Since the 1990's the necessity to describe MSA assemblages from a technological perspective by identifying reduction sequences was emphasised (Wurz, 2000; Wurz, 2002; Porraz et al., 2013b; Will et al., 2013; Douze et al., 2015; Schmid et al., 2016). Recently, a number of new studies have been published about the MIS 5 lithic technology, for example at Blombos Cave (Douze et al., 2015), Border Cave (Backwell et al., 2018), Bushman Rock Shelter (Porraz et al., 2018), Diepkloof (Porraz et al., 2013b), Elands Bay Cave (Schmid et al., 2016), Hoedjiespunt (Will et al., 2013), the Pinnacle Point sites 13B and 5–6 (Thompson et al., 2010; Brown, 2011), Putslaagte (Mackay et al., 2015) and Sibudu (Rots et al., 2017). What seems clear is that MIS 5 technology varies greatly between different sites especially in terms of reduction sequences. MIS 5 does not only span an extended time period (from about 125–74 ka), but sites are dotted throughout the country. A number of inland sites in the north-eastern provinces (Border Cave, Bushman Rockshelter, Florisbad, Sibudu) coexist with coastal and inland sites in the Western Cape (Die Kelders, Diepkloof, Elands Bay Cave, Hoedjiespunt, Putslaagte, Ysterfontein) and Southern Cape (Blombos, Cape St Blaize, Klasies River, Pinnacle Point). Mackay et al. (2014) did suggest that there are broad

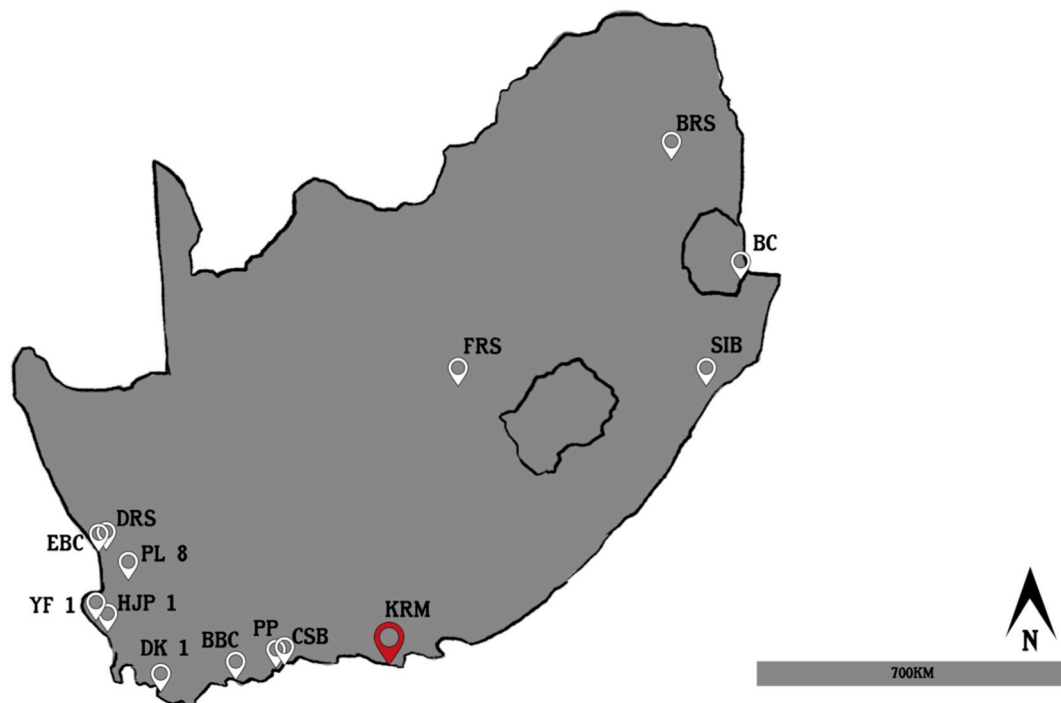


Fig. 1. Map with all the mentioned sites. Blombos Cave (BBC), Border Cave (BC), Bushman Rock Shelter (BRS), Cape St Blaize (CSB), Die Kelders 1 (DK 1), Diepkloof (DRS), Elands Bay Cave (EBC), Florisbad (FRS), Hoedjiespunt 1 (HJP 1), Klasies River (KRM), Pinnacle Point (PP), Putslaagte 8 (PL 8), Sibudu (SIB), Ysterfontein 1 (YF 1).

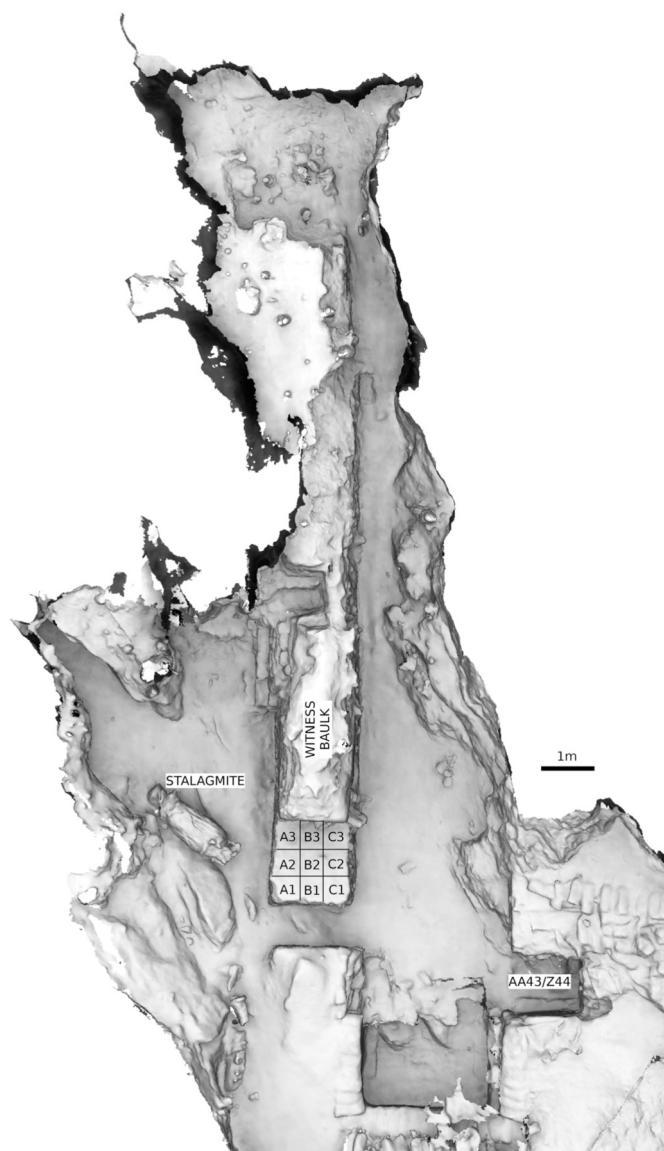


Fig. 2. Klasies River main site Cave 1. 3D model of the site with the Witness Bulb in the centre of the cave. The excavation grid with squares A1 - C3 shows the area where the material discussed in this paper originate from (image courtesy of the Zamani project).

technological similarities between the various sub-regions from South Africa, but as we discuss for MIS 5 sites from the southern Cape in Section 4, at this point it is complex to understand how the sites relate to each other from a technological perspective. In spite of increased focus on lithic technology from MIS 5 assemblages from South African sites, it is not as well understood as the more intensively studied techno-complexes from MIS 4, which include the Still Bay and Howiesons Poort. This may be because these phases are characterized by a richer formal tool component in comparison with MIS 5 industries, with tools such as Still Bay points, geometrically backed pieces and distinctive notched artefacts.

MIS 5 lithic material is usually studied concerning units of deposit that reflect extended periods of time. The MIS 5 assemblages from KRM come from > 12 m of deposits. Singer and Wymer (1982) and later also Thackeray (Thackeray and Kelly, 1988; Thackeray, 1989) grouped all of the lithic material of the SAS member into the MSA II, and that of the LBS member into the MSA I. Wurz also divided the MIS 5 lithic material from KRM into two different techno complexes but termed them the Klasies River (MSA I) and the Mossel Bay (MSA II) techno-complexes.

These terms are used interchangeably in the literature together with Volman's (1981) MSA 2a for the former and MSA 2b for the latter. In this paper, the terms MSA I and MSA II are used as these were the original labels. The MSA I shows the co-existence of two reduction systems, a laminar production on pyramidal cores and a Levallois production system. The blade and point end products are described as thin and symmetrical with a curved profile (Wurz, 2002, p. 1005). The MSA II is characterized by a unidirectional convergent Levallois method for the production of points. The majority of the blades are thicker and more irregular compared to the MSA I blades (Wurz, 2002, p. 1008). Wurz (2002), recognized differences between an upper and a lower MSA II, especially in the morphology of points. In the upper MSA II, the points are smaller in all dimensions (Thackeray and Kelly, 1988, p. 20; Wurz 2000, p. 79).

Our aim is to explore whether the analysis of fine-grained chrono-stratigraphic units from the MSA II at KRM results in a deeper understanding of the internal variability of the MSA II and whether this may provide a way to more efficiently link to other MIS 5 assemblages. The results of the technological analysis of two recently excavated layers from the lowermost part of the MSA II at KRM are reported here.

2. Archaeological sample and method

The lithic samples discussed here originate from the Wurz excavations of the Witness Bulb (Fig. 2). The Witness Bulb contains Layers 38, 37, 17-14 of Singer and Wymer (1982, hereafter abbreviated to SW) that were labeled as five members by Deacon (Deacon and Geleijnse, 1988, Fig. 5). The lowermost members include the Layer 38 (SW) or the Light Brown Sand (LBS) member and Layer 37 (SW) or Rubble Brown Sand (RBS) member (see Fig. 3). The RBS member is currently under study from sedimentological and micromorphological perspectives, and this designation within the Witness Bulb may change (Wurz et al. in prep.). The overlying Layers 17-14 (SW) or Shell And Sand (SAS) and White Sand (WS) members are topped by a Later Stone Age shell midden (Fig. 3). The SAS member consists of sub-members SAS Rubble (SASR, SW Layer 14), SAS Wedge (SASW, SW layer 15) SAS Upper (SASU, SW Layer 16) and SAS Lower (SASL, SW Layer 17a and b). Fig. 7 of Deacon and Geleijnse (1988) refers to SASL in the Witness Bulb as SASB, but subsequently, this was changed to SASL (Wurz, 2002; Deacon, 2008). The SAS member in Cave 1A with 10 m of deposit, is much more extensive than in Cave 1. Deposits that accumulated in Cave 1A sloped into Cave 1 and formed the SASW sub-member (SW Layer 14). The artefacts from this unit relate to the MSA II upper (Wurz, 2000). The SASU and SASL sub-members consist of deposits that formed by groups living within Cave 1 and are associated with MSA II lower artefacts (Wurz, 2000). The underlying RBS and LBS members contain MSA I artefacts (Wurz, 2002).

The focus of this paper is on the lithic artefacts from the SASL sub-member of the Witness Bulb, excavated in 2015 and 2016. This excavation continued from where the Deacon excavations ended in 1995. The horizontal extent of the excavation area is 1.7×1.7 m (2.89 m²). Excavation protocols include the piece plotting of all artefacts > 20 mm and frequent photographic recording of small-scale quadrants, as well as the whole excavation surface. At the site all material was dry sieved with 5 and 2 mm meshes, and the resultant coarse and fine fraction further wet-sieved in the laboratory.

The newly excavated SASL sub-member consists of layer SMONE (Shell Midden One), equivalent to Singer & Wymer's Layer 17a (Wurz et al., 2018), and the Black Occupational Soils layer BOS, which is equivalent to Singer and Wymer's Layer 17b (Fig. 4). In Table 1, the layers and volume of deposit for SMONE and BOS are presented. Lithics, shellfish and fauna larger than 2 cm as well as tufa and non-artefactual quartzite that show signs of heat alteration have been piece-plotted and removed prior to measurement of the volume of the excavated sediment.

There are clear differences between SMONE and BOS. Singer &

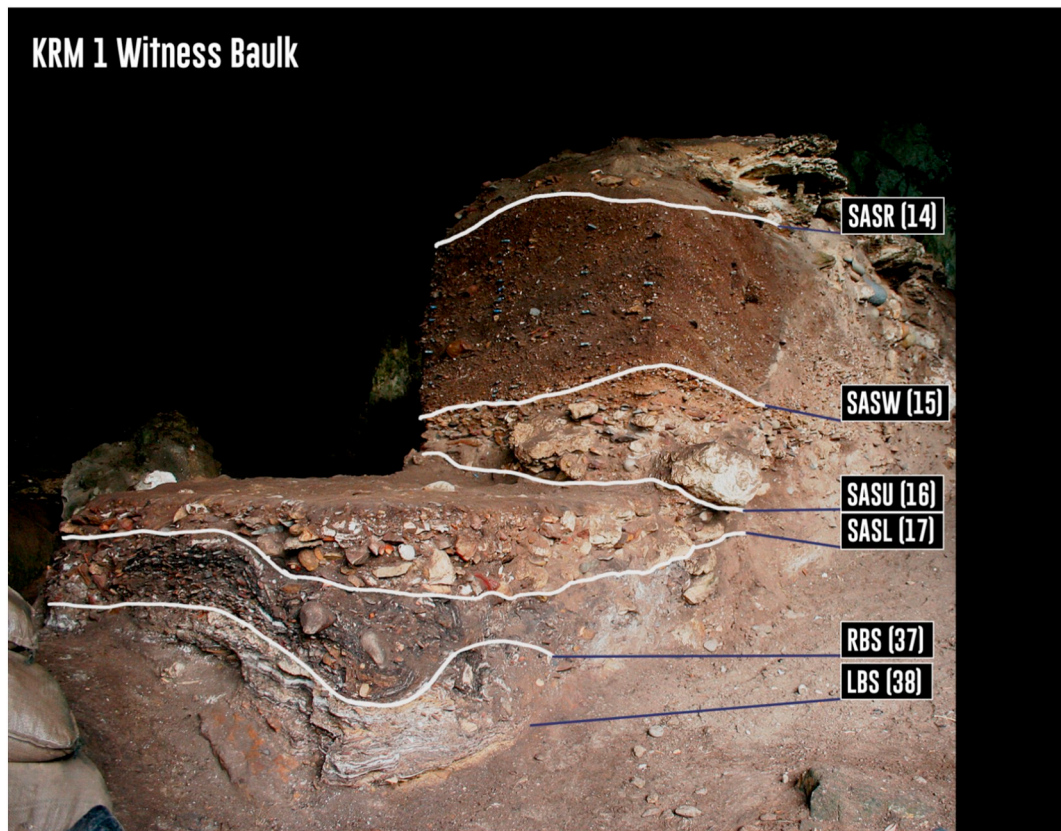


Fig. 3. KRM Cave 1 Witness Baulk. Deacon's designation for the members with Singer and Wymer's layer number in brackets.

Wymer (1982, p. 26) describe layer 17a as a 'tumble layer', and the current excavation confirmed this. The 2015 excavation revealed the SMONE layer in the Witness Baulk to be a wedge of deposit that is up to 15 cm thick in the eastern part and thins out to ca 5 mm in the western part of the Witness Baulk. The deposits consist of a soil and rubble matrix with artefacts and other finds evidencing a palimpsest. The matrix further contains disintegrated tufa blocks, small leached ash

patches, and small charcoal pieces with no in situ combustion features. An interesting feature is quartzite rocks, which display colour changes, fractures and other signs of being exposed to fire (Bentsen and Wurz, 2017).

In contrast, BOS are 'occupational soils' (Singer and Wymer, 1982, p. 26). The current excavations confirm this observation, but BOS is also a palimpsest. No in situ combustion features occur here either,

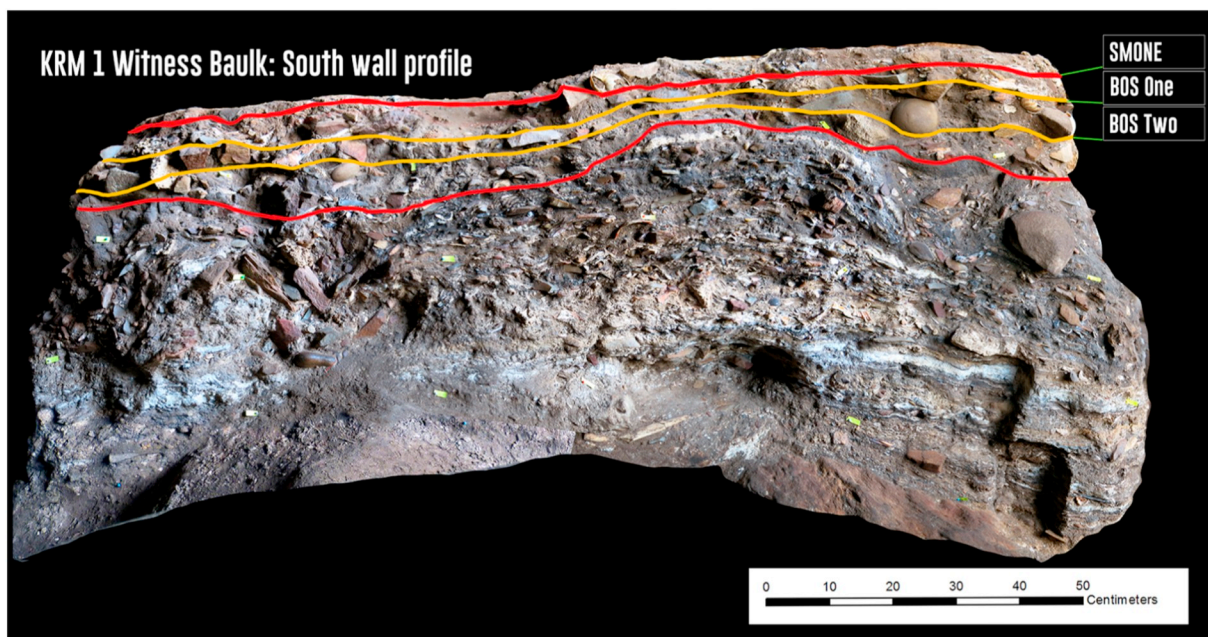


Fig. 4. South profile of the Witness Baulk indicating the layer SMONE and spits one and two of layer BOS excavated between 2015 and 2016, discussed in this paper.

Table 1

Volume of excavated deposit in m³, total number of lithic artefacts per layer and density in artefact numbers per liter.

Layer	Volume of deposit excavated (m ³)	Lithic artefacts (n)	Density (artefacts per liter)
SMONE	0.054	2671	50
BOS	0.078	4032	52

although large patches of leached ash associated with burnt quartzites (Bentsen and Wurz, 2019) occur. There is also a much more pronounced presence of tufa material, many in the form of large blocks, that cemented some of the archaeological remains associated with BOS. Shell preservation is excellent in pockets and the preservation of bone, many of which are from large mammal fauna, is also very good. Although many of these finds are in situ and preserved in anatomical detail, they show crushing, perhaps from weight of overlying deposit in combination with removal of supporting sediment through leaching. The taphonomic study of the bone in process (Reynard et al. in prep) and the moist, fine clayey nature of the deposits indicate possible water action.

Our excavation of the BOS layer is in progress, and it is divided into arbitrary spits with BOS One about 10 cm thick, and BOS Two around 7 cm, although the presence of large tufa blocks in the deposit precludes an accurate estimation of thickness. The nature of the soils and preservation pattern indicate that BOS One and BOS Two are parts of the same depositional period and therefore these spits are analysed as one layer, BOS, here.

Current dating of the Witness Baulk bracket the deposits between 85 ka and 115 ka. Layer 14 SW (the SASR sub-member of Deacon), 2 m above the SASL sub-member, was dated with U-Th on stalagmites, giving ages of 85.2 ± 2.1 , 94.6 ± 3.2 ka and 100.8 ± 7.5 ka (Vogel, 2001). U-Th dating of flowstone that grew on the ceiling of Cave 1 and fell into the base of the SASU sub-member (Deacon's Layer HHH (Wurz, 2000)), was undertaken by Pickering and Green (Wurz et al., 2018). This provides an age of 126.0 ± 1.5 ka and a maximum age for the SASU deposits. A bovid tooth from Singer & Wymer's Layer 17b has an ESR date of 102–63 ka (early uptake model) and 104–64 ka (linear uptake model) (Millard, 2008) and a U-series/ESR estimate of 101 ± 12 ka (Eggins et al., 2005). An age of 100,000 years ago can thus be regarded as a minimum age of the SASL deposits. Other dates available for the lowermost part of the sequence are for the LBS member that, on current evidence, are associated with ages of between 108.6 ± 3.4 ka (Vogel, 2001) and 106.8 ± 12.6 ka (Feathers, 2002). Layer SMONE, thus certainly older than 100 ka, probably dates to within MIS 5c (93–106 ka, MIS boundaries according to Wadley, 2015). Our designation of the BOS layer to MIS 5d (115–106 ka) is based on new uranium-series ages from in situ BOS stalagmitic material dating to within this period (Pickering pers comm; Wurz et al. in prep., Mentzer et al. in prep).

3. Results

3.1. Assemblage composition

The lithics from all of the layers discussed here consist mainly of quartzite, and they have a similar assemblage composition. The total lithic artefacts are 2671 in SMONE, 4032 in BOS (Table 1), whereas the pieces > 20 mm comprise 609 in SMONE and 1244 in BOS (Table 2). The small debitage is somewhat more numerous in the upper layer SMONE with 77.2% of the whole assemblage compared to BOS with 69.2% small debitage.

Flakes constitute the highest percentage of detached debitage in both assemblages, with 24% and 17.3% complete flakes, in addition to 27.9% and 24.5% fragments in SMONE and BOS respectively (Table 2).

Blades and points are more numerous in the lower layer (2.1% blades and 5.7% points in SMONE, 3.9% blades and 10.3% points in BOS). The bladelet component shows a decrease from the top with 7.8% in SMONE to 3.3% in BOS. The cores are less numerous in the upper layer SMONE (1.8%) than in the lower layer BOS (4.3%). The hammerstones show the same pattern as the cores, they are least common in SMONE (0.5%) and most abundant in BOS (2%) (Table 2).

3.2. Raw materials

The raw materials from Klasies River were visually inspected based on their macroscopic mineral content; they include quartz, quartzite, altered quartzite, Table Mountain Sandstone, sandstone, silcrete and indeterminable other raw material. Table 2 shows the detailed raw material composition for pieces > 20 mm; the counts of the small debitage < 20 mm indicate only the collective amount of the different quartzite types.

The source or parent rock of Cave 1 is Table Mountain Sandstone, which is a quartzite of the Cape Supergroup. It is coarse-grained, has poor knapping qualities and is present mostly as chunks and flakes making up 1.8–9.2% of the assemblages (Table 2). The raw material used at Klasies River is dominantly quartzite from cobbles and pebbles. It is highly probable that the quartzite was available locally (< 5 km) from beaches and the close vicinity of Klasies River as the shore remained close to the site during MIS 5 (Van Andel, 1989). A medium-grained quartzite is the most frequently occurring raw material (82.2–88.8%). Several quartzite artefacts have been labeled “altered quartzite” (highest amount in BOS, 4.6%) because they have a rough surface appearance (on both the cortex and the flake scars) and reddish, rust-like spots covering the surface (e.g. Fig. 5). It is possible that post-depositional alteration has caused this, but this hypothesis is under investigation. Sandstone is the next most abundant raw material for pieces > 20 mm with frequencies of 2.1–2.3%. Some of the sandstone pieces show cobble cortex, attesting a river or beach source.

Quartz does not occur in notable frequencies in pieces > 20 mm with only 1.3% in SMONE and 1.1% in BOS. Nevertheless, it is more abundant in the small debitage < 20 mm (8.3% in SMONE and 20.4% in BOS), which results in relatively high percentages of quartz in the assemblage composition when the small debitage is included (6.7–14.5%). It seems that the same core reduction strategies were followed as for quartzite. Very few pieces of silcrete are present with 0.2% in SMONE and 0.1% in BOS, including pieces < 20 mm).

3.3. First reduction of cobbles

A relatively large proportion of the lithics > 20 mm show cortex, which is water rounded cobble cortex. Cortex cover occurs more often in BOS (38.7% of artefacts > 20 mm) than in SMONE (28.4%). The cobbles were most probably opened by splitting them with a bipolar on anvil technique (see, e.g. Shott and Tostevin (2015)) as evidenced by crushing marks and radiating striations from the impact point on 13 artefacts in the assemblages (Fig. 6). It could have happened at the beach, or, as the presence of two anvils in the SMONE assemblage attests, in the cave.

The further reduction of unworked split cobbles was conducted in the cave, as shown by the presence of all of the steps of the reduction sequence. The first phase of reduction entailed opening the split cobble core blank by removing debordants or core edge flakes, showing a cortical side and the surface of a split cobble. A few first flakes (*entames*) with cortex on their dorsal side and platform are part of the assemblage as well ($n = 1$ in SMONE, $n = 3$ in BOS).

3.4. Knapping technique

All of the quartzite debitage show clear signs of free-hand percussion with a hard hammer, as prominent bulbs (Table A.1) with a

Table 2
Assemblage compositions by category and raw material of SMONE and BOS.

Raw material/ category	Quartz	Quartzite	Altered quartzite	Table Mountain Sandstone	Cobble sandstone	Silcrete	Other	Total	% of > 20 mm per assemblage
Blade									
SMONE		13						13	2.1%
BOS		49						49	3.9%
Bladelets and bladelet fragments (including < 2cm)									
SMONE	2	47						49	1.5% ^a
BOS	1	40			1			42	0.7% ^a
Point									
SMONE		35						35	5.7%
BOS	1	127						128	10.3%
End product fragment									
SMONE		63	1					64	10.5%
BOS		197	1	1	2			201	16.2%
Flake									
SMONE		131	7		2		1	146	24%
BOS	1	191	5	8	3		2	215	17.3%
Indeterminate fragment									
SMONE	2	154	9	1	3	1		170	27.9%
BOS		281	9	11	3	1		305	24.5%
Core									
SMONE		11						11	1.8%
BOS	2	42	8	2				54	4.3 %
Hammerstone									
SMONE	3							3	0.5%
BOS	19		5	1				25	2.0%
Chunk									
SMONE	5	123	9	10	8		8	163	27.9%
BOS	9	109	29	92	19		3	258	20.7%
Total > 2cm									
SMONE	8	541	26	11	13	1	9	609	100%
BOS	14	1022	57	115	28	1	5	1244	100%
% of total > 2cm									
SMONE	1.3%	88.8%	4.3%	1.8%	2.1%	0.2%	1.5%	100%	
BOS	1.1%	82.2%	4.6%	9.2%	2.3%	0.1	0.4%	100%	
Small debitage < 20 mm									
SMONE	172	1884				5		2062	
BOS	569	2221						2790	
Grand Total									
SMONE	180	2425	26	11	13	6	9	2671	
BOS	583	3243	57	115	28	1	5	4032	
% of total									
SMONE	6.7%	90.8%	1.0%	0.4%	0.5%	0.2%	0.3%	100%	
BOS	14.5%	80.4%	1.4%	2.9%	0.7%	0.1%	0.1%	100%	

^a Percentage of bladelets including < 20 mm: SMONE 7.8%, BOS 3.3%.

contoured Hertzian cone, as well as well-developed ring cracks at the point of impact (Table A.2) attest. The platforms are rather thick (Table A.3), and the exterior platform angle is very wide, close to 90° (Table A.4). Furthermore, attributes that might have indicated soft hammer percussion, e.g. platform rubbing (Table 12 for blanks) and well-defined lips (after Andrefsky, 2005, p. 18) are rare (Table A.5; 3.7% in SMONE; 1.7% in BOS). These characteristics speak for hard hammer direct percussion.

3.5. Technological analysis of the blanks

The blanks can be divided into preparational pieces and end products (Table 3). The term “end product” is used in the sense of for example Douze et al. (2015), acknowledging the caveats associated with such a premise (Dibble et al., 2017, p. 2) as archaeologists cannot identify the ‘emic’ connotation and meaning of artefacts (Bar-Yosef and Van Peer, 2009). They are predominantly regular in shape and dorsal scar pattern (following Damlien, 2015, Fig. 8). The end products form

between 21.2% in SMONE, 34.6% in BOS of all complete debitage (Table 3) and are discussed in more detail below.

The pointed products of KRM have been described variously in previous studies as “pointed flake-blades” (Singer and Wymer, 1982, p. 56), “convergent flake-blades” (Thackeray, 1989, p. 39) and “points”. Here we follow Wurz’s terminology, in that all pointed products are called points. This includes convergent blanks (symmetric and asymmetric) and pieces with a pointed tip but otherwise parallel edges (further explanation below). Blades are all products with a length-width ratio of at least 2:1 and parallel or sub-parallel edges (e.g. Crabtree, 1972), excluding pointed pieces and pieces of bladelet dimensions. Bladelets have a similar length-width ratio with parallel edges and, as defined by Tixier (1963) and Deacon (1984, p. 525), have a width of up to 12 mm. Flakes are all detached pieces that have a smaller length to width ratio than 2 and show any shape, except a triangular shape or a pointed tip.

The preparational flakes (details in Table 3) are either for setting up cores, such as *entames* and decortification flakes, or they are adjusting



Fig. 5. Altered quartzite core #2829 from BOS. It shows a rough surface and red-brown staining.

the core convexities. Lateral convexities are set up by the removal of debordants or core edge flakes. Debordants usually show a lateral or central arris with one side fully or partly cortical, although in some cases, no cortex is seen, but negatives from other lateral preparation. Core surface management pieces restore the core surface, e.g. to remove step fractures or to create arrises for the subsequent removal. Platform shaping flakes can be trimming flakes or pieces removing bigger parts or the core platform, in order to adjust the edge angle. Flaking debris are smaller flakes, around 20 mm ($n = 66$), which are probably waste from knapping, this category also includes indeterminate pieces and flakes which could stem from the opportunistically exploited second generation cores discussed above (see unsystematic core reduction, Fig. 20).

Flakes are the most numerous blank type, and Table 3 clearly shows that they are predominantly related to preparation phases, with the highest amount of core surface management flakes, followed by de-certification flakes, debordants and platform shaping flakes. Points are the second most frequent blank type with most of the points interpreted as end products ($n = 21/35$ in SMONE, $n = 94/131$ in BOS), although debordants are also common (Table 3). The blades and bladelets occur least frequently. Most of the blades are end products ($n = 7/13$ in SMONE, $n = 21/50$ in BOS), although a relatively high amount (5/13 blades in SMONE, 14/50 in BOS) are debordants (Table 3). There are only four complete bladelets longer than 20 mm in SMONE, and they are either categorized as core surface management or debris, due to their thickness and shape. There is, however, a definite bladelet production component in the assemblage as attested by the removal traces on the cores and bladelets/bladelet fragments < 20 mm (Fig. 19: $n = 4$ cores, Table 2: $n = 91$ bladelets).

3.5.1. End product morphology

The end products of the SMONE and BOS layer differ in many respects, as discussed below. Student t-tests (t) (for data with normal distributions) and Mann-Whitney U tests (U) (for data that are not normally distributed) were undertaken to compare continuous variables between the layers. Chi-square tests (were undertaken to quantify comparisons between categorical variables).

End products comprise flakes, blades and different types of points (Fig. 7). The points form the most numerous component of the end products, and as other researchers might not group all the morphologies termed here as points into that category, we describe them in more

detail in separate point categories to enable comparisons to other sites. All of the KRM points can be categorized into one of the following three morphological types (Fig. 7a–c, Table 4).

Type 1 (Fig. 2, Fig. 7, Table 4) is the most common type and is represented by flake sized triangular flakes with symmetrical or skewly/asymmetrical converging edges (Table 4: 52.4% in SMONE, 69.1% in BOS; Fig. 8a–c). Type 2 points (Table 4: 33.3% in SMONE, 21.3% in BOS) also show converging edges but have blade dimensions (Fig. 8d–e). Type 2 is most common in SMONE. Some of the types 1 and 2 points here, resemble Levallois points (after, e.g. Thompson et al., 2010; Porraz et al., 2013b; Douze et al., 2015). The type 3 points are less frequent (Table 4: 14.3% in SMONE, 9.8% in BOS), and they are characterized by parallel edges and a pointed tip (Fig. 8f and 12e). This type is mostly found on blade sized pieces. Apart from the blade sized points, the blade end products are mostly regular to very regular, which means they have parallel to sub-parallel lateral edges and display mostly parallel dorsal negative scars (following Damlien, 2015). The blades are present in low numbers, with the higher proportion seen in BOS (Fig. 8h–i, Table 3).

The flake end products are rare (Table 3) and SMONE, which has the most flake debitage, also shows the most flake end products (6.3%). The flake shapes are mostly rectangular (Fig. 8g); some are also round/oval, expanding or irregular (Table A.7). Bladelets occur as well (Fig. 10). The complete and fragmentary bladelets form a small component in the assemblages, with the highest number in SMONE (7.8%) and lower frequencies in the BOS assemblage (3.3%; Table 2, Fig. 10). The bladelets interpreted as end products are regularly shaped with parallel edges and a width of between 4 and 10 mm. Of bladelets with preserved proximal ends, plain platforms ($n = 9$) are as frequent as faceted or informal faceted ones ($n = 9$), with only one bladelet showing a cortical platform. The same is seen regarding the profiles of the bladelets, nine show a twisted or curved profile, and nine have a straight profile. There is no correlation between profiles and platform preparation. It is, however, highly likely that the bladelets have been produced using a separate reduction sequence, as the distribution of width of blades and bladelets shows a bimodal distribution (Fig. 9). Bladelet cores were identified only in BOS (Fig. 19s).

The weight of the end products varies between the SMONE and the BOS assemblages (Table 5). In SMONE all end product types are lighter than in BOS (average weight for SMONE points 21.7 g, blades 24 g and flakes 17.8 g). In BOS the points and blades have a mean weight of ca.



Fig. 6. Artefacts with a split cobble surface showing crushing and striation marks. The dotted surface represents cortex. All on medium grain quartzite. a) core #3241, BOS; type IV core; b) point #249, SMONE, debordant with one cortical side and one side showing the crush marks from splitting a cobble; c) core #1076, with rusty staining on cortex, SMONE, type III core; d) blade refit #1607 and #2225, BOS, debordant with one cortical side and one side showing the crush marks from splitting a cobble.

30 g (points 29.7 g and blades 30.4 g). The flakes of BOS (37.3 g) are on average heavier than the other blank types. A student's *t*-test reveals that the points from SMONE and BOS are significantly different in weight ($p < .05$).

Many of the products are much longer than any of the cores (Table A.6 core dimensions), hinting at long reduction sequences and intensive reduction of the cores. The average length of each end product type is very similar in both assemblages (Table 5, Fig. 11a). The length of blades seems to be less variable in SMONE, but this observation is preliminary as the numbers of blades are very low in all assemblages (n between 7 and 21). The point end products are more numerous and have a similar length in both assemblages. It appears that the platform thickness (Fig. 11b) shows a more apparent distinction between the SMONE and the BOS assemblages, with both the blade and point end products, having thicker platforms in BOS, than in SMONE. However, the *t*-tests attest no statistical significance ($p > .05$). The length/width ratios (Table 11c) of points and blades also show no significant difference between the two layers when a Mann-Whitney *U* test is used ($U = 791, p > .05$).

All of the end products have straight profiles with thick, prepared,

mostly trapezoid shaped platforms. The platforms are predominantly prepared (of pieces with preserved platforms: SMONE 82.4%, BOS 87.1%) (Table 6; also see Table A.8 for all blanks). The term 'informal faceting' is used to describe platforms which do not have clear facet negatives, but show little trimming and step flaking on the platform from the dorsal edge. In SMONE informal faceted platforms, with little trimming and step flaking on the platform, is most common, but formal faceting occurs frequently as well. In BOS the formal faceted platforms are most frequent, followed by informal faceted platforms. In all the assemblages, about half of the blanks are without proximal preparation of the dorsal edge. Table 7 shows that step flaking of the proximal edge is quite common (33.3% in SMONE, 39.3% in BOS) and a more invasive preparation with longer removals along the dorsal scar ridges is found on about 10% of the end products in both layers. Rubbing as part of preparation is very scarce and occurs in only 0.2–4.3% of the cases (Table 7). The external platform angle (EPA) for the end products measures close to 90° (see Table A.4 for all detached pieces). In order to detach large pieces at such a wide angle, the platform needs to be thick (Speth, 1981; Pelcin, 1997; Dibble and Rezek, 2009). Variation is seen between SMONE and BOS, with blades and points in SMONE having

Table 3
Technological categories of complete blanks > 20 mm in the two assemblages.

Technological category/ blank	End product		Debordant fully cortical		Debordant partly cortical		Debordant other		Core surface management		Platform shaping		Decortification flake		Entame (first)		Flaking debris		Total	
	n	%	n	%	n	%	n	%	n	%	n	%	n	%	n	%	n	%	n	%
SMONE																				
Points	21	11.1%	5	2.6%	4	2.1%	3	1.6%	3	1.6%	-	-	-	-	-	-	1	0.5%	37	19.6%
Blades	7	3.7%	2	1.1%	1	0.5%	2	1.6%	1	0.5%	-	-	-	-	-	-	-	-	13	6.9%
Bladelets	-	-	-	-	-	-	-	-	3	1.6%	-	-	-	-	-	-	1	0.5%	4	2.1%
Flakes	12	6.3%	15	7.9%	2	1.1%	1	0.5%	37	19.6%	16	8.5%	18	9.5%	-	-	34	17.9%	135	71.4%
Total SMONE	40	21.2%	22	11.6%	7	3.7%	6	3.2%	44	23.3%	16	8.5%	18	9.5%	-	-	36	19.0%	189	100%
BOS																				
Points	94	24.3%	18	4.7%	7	1.8%	1	0.3%	8	2.1%	1	0.3%	1	0.3%	-	-	1	0.3%	131	33.9%
Blades	21	5.4%	14	3.6%	4	1.0%	1	0.3%	9	2.3%	-	-	-	-	-	-	-	-	50	12.9%
Flakes	19	4.9%	17	4.4%	5	1.3%	3	0.8%	74	19.1%	19	4.9%	36	9.3%	2	0.5%	31	8.0%	206	53.2%
Total BOS	134	34.6%	49	12.7%	16	4.1%	5	1.3%	91	23.5%	20	5.2%	37	9.6%	2	0.5%	32	8.3%	387	100%
Grand total	174	30.2%	71	12.3%	23	4.0%	11	1.9%	135	23.4%	36	6.3%	55	9.5%	2	0.3%	66	11.4%	576	100%

narrower EPAs, closer to 80° on average than in BOS where EPAs are closer to 90° (Table A.4). The difference between layers is, however, only statistically significant for the blades as attested by a Mann-Whitney U test ($U = 436, p < .05$).

Almost none of the end products show remains of cortex, and in the few cases where it is present, it is < 10%. A large percentage of the end products show a unidirectional dorsal scar pattern (Tables 8, 63.9% in SMONE and 54.1% in BOS). This high number confirms the impression from the cores that the main reduction system is unidirectional. The scar shapes indicate convergent (Table 8: $n = 3$ in SMONE, $n = 20$ in BOS) and parallel reduction ($n = 3$ in SMONE, $n = 14$ in BOS). End products with some distal preparation from an opposed platform have a 90% unidirectional scar pattern (with some bidirectional scars on the distal end, $n = 9$ in SMONE, $n = 15$ in BOS). The bidirectional dorsal scar pattern rarely occurs in SMONE ($n = 6$) but is more abundant on blanks in BOS ($n = 31$).

3.5.2. Tools and edge damaged pieces

The formal tool types are denticulates, notched pieces, scrapers and laterally retouched pieces (Fig. 13). Laterally retouched pieces have regular retouch negatives in a restricted area of the lateral edge, which are not sufficiently continuous to be classified as a side-scraper. Formal tools occur in low proportions in both assemblages (in relation to pieces > 20 mm: 0.7% of SMONE, 2.8% of BOS). The main tool types are denticulates and notched pieces (Table 9). SMONE has fewer tools ($\chi^2(1) = 8.91, p < .05$) and shows less variety in tool types. The tools of SMONE are all fragmentary but include three notched pieces and one denticulate on a point. BOS contains seven notched pieces (mostly flakes), eight denticulates, nine pieces with lateral retouch (mostly points) and seven scrapers (Fig. 12, Table 9). Four of the scrapers are on thick core blanks (Fig. 13), the other three are on different blank shapes, including points, blades and flakes. The working edges of the scrapers are mostly convex (Figs. 12b and 13), and only one piece shows a concave working edge.

Three tools from BOS show scraper retouch and notching in combination and all of them are on flake blanks (Table 9). Additionally, heavy-duty scraper damage can be seen on some thick pieces in BOS, which are often core preparation flakes or debordants (Fig. 14f-g). This may speak to some opportunistic utilisation of lithics which are by-products, for example in the early stages of butchering when robust and heavy tools are needed.

A number of pieces have been classified as ‘edge damaged’ (Table 9). Edge damage does not resemble intentional retouch, as the scars are irregular in their shape and distribution and might have developed through use. Edge damage traces have been identified, macroscopically and microscopically under low magnification (40×). This type of damage has also been referred to as “informal retouch” by Douze et al. (2015). Post-depositional processes may have caused this, but there is no indication of abrasion on the dorsal scar ridges of the lithics. The number of pieces with edge damage exceeds those with formal retouch. In SMONE, 16.4% of the assemblage exhibit edge damage, and in BOS, the frequency is slightly higher with 21.7% (Table 9). SMONE shows no preference for shape, as edge damage occurs almost equally on point, blade and flake blanks. In BOS the points have the highest occurrence of edge damage traces with 9.4% (Table 9). This indicates a preference for pointed pieces being used as tools, which is confirmed by a chi-square test ($\chi^2(1) = 11.56, p < .05$).

SMONE shows the least amount of formal tools (0.7%) and edge damage (16.4%), whereas BOS exhibits higher frequencies of formal tools (2.8%) and edge damage (21.7%). The frequency of formal tools is very low and the higher amount of edge damage in both assemblages implies that mostly unretouched blanks were used as tools. In SMONE there is no preference of blank shape for the use as tools, but in BOS edge damage is dominantly seen on points.

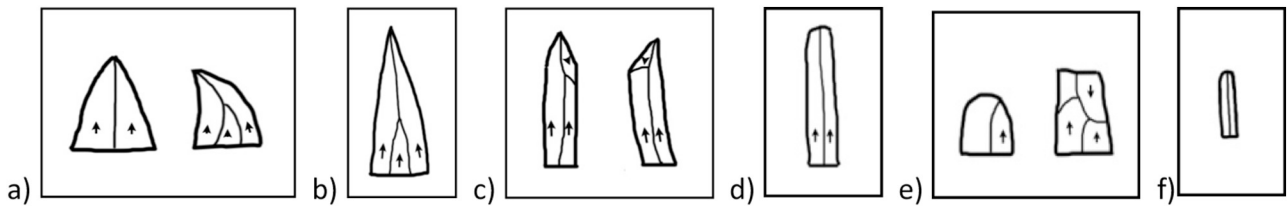


Fig. 7. End product types a) point type 1; b) point type 2; c) point type 3; d) blade; e) flake; f) bladelet.

Table 4
Point categories per assemblage (only complete points).

Point category/layer	Type 1		Type 2		Type 3		Total	
	n	%	n	%	n	%	n	%
SMONE	11	52.4%	7	33.3%	3	14.3%	21	100%
BOS	65	69.1.4%	20	21.3%	9	9.8%	94	100%
Total	76		27		12			

3.6. Core analysis

The purpose of this section is to describe the different core types and the related *chaîne opératoires* present in the analysed assemblages (see Figs. 15–16 and Tables 10–12). The core blanks are predominantly cobbles or cobble fragments (Table 10). Two of the cores with cobble origin also show pit marks, which evidence a primary use as a hammerstone. Additionally, debordants and flakes have been used as core blanks. There are some indeterminate cases where the core blank was

unclear.

The cores ($n = 65$) have been classified into platform ($n = 5$), parallel ($n = 18$), bladelet core ($n = 4$), tested ($n = 11$) and indeterminate ($n = 17$) whereas 10 pieces are indeterminable fragments of cores (Table 11). A detailed description of core types is given below. Table 12 shows the core categories according to type, morphology, the orientation of negatives and the products removed.

3.6.1. Type I: platform cores

The type I cores comprises unidirectional platform cores with only one platform ($n = 5$; Table 11). The platform cores follow a type of volumetric system, in which predetermined products are removed in a recurrent manner. Most platform cores show a reduction surface “around a corner” (Conard, 2012), which resembles semi-rotational reduction. The geometry of the platform cores varies between pyramidal and prismatic (after (de Sonneville-Bordes, 1960; de Heinzelin de Braucourt, 1962; Brezillon, 1968).

In SMONE two cores are classified as type I. BOS comprises two type I platform cores with a prismatic morphology and parallel negative

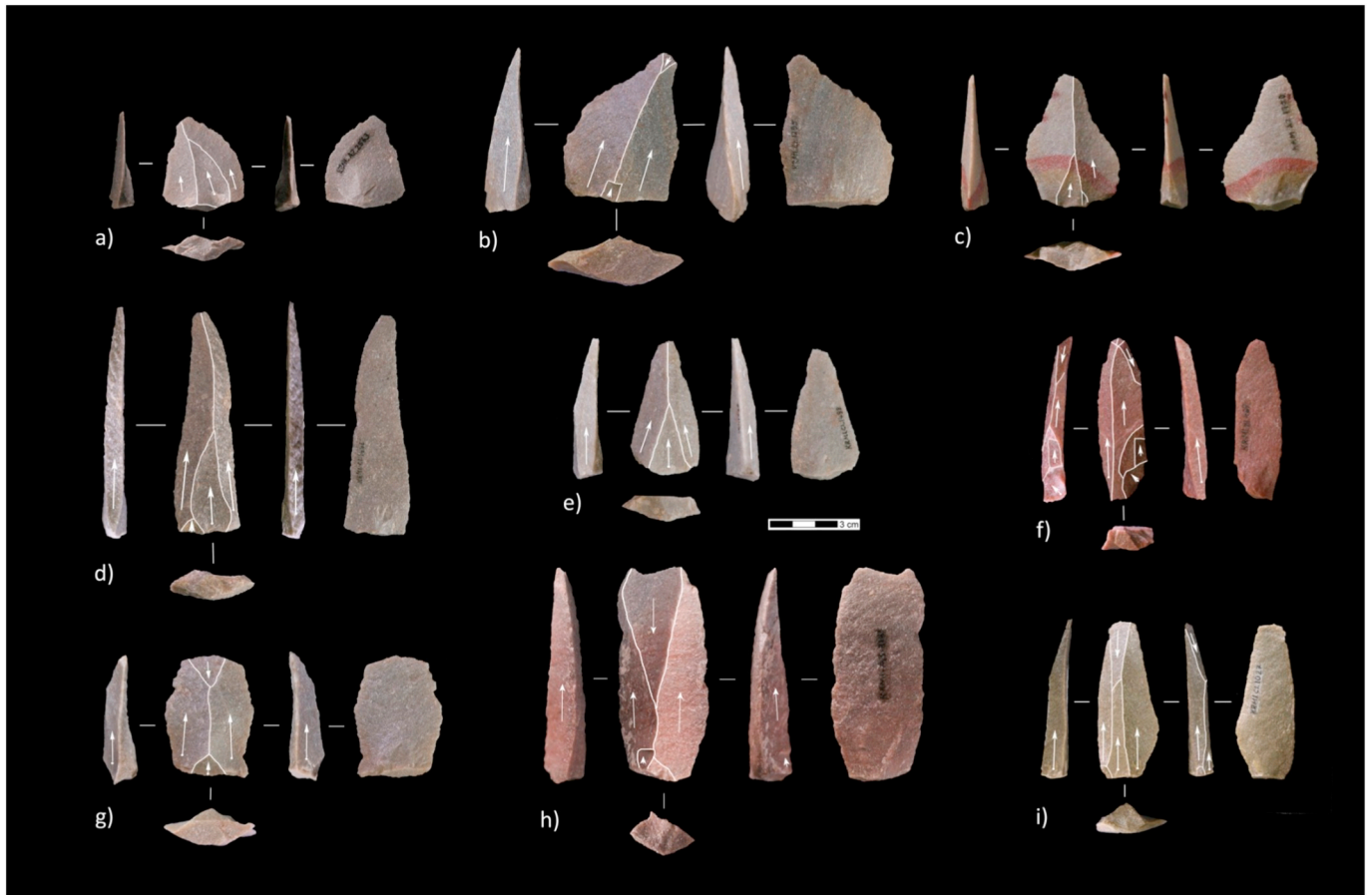


Fig. 8. KRM end products. All in medium grain quartzite; a) type 1 point #2563, BOS, Levallois-like; b) type 1 point #1595, BOS, with edge damage; c) type 1 point #1900, BOS, Levallois-like; d) type 2 point #1446, SMONE, Levallois-like; e) type 2 point #1498, SMONE, Levallois-like; f) type 3 point #467, SMONE; g) type 3 point #255, SMONE; h) blade #3181, BOS, with edge damage; i) blade #1027, SMONE.

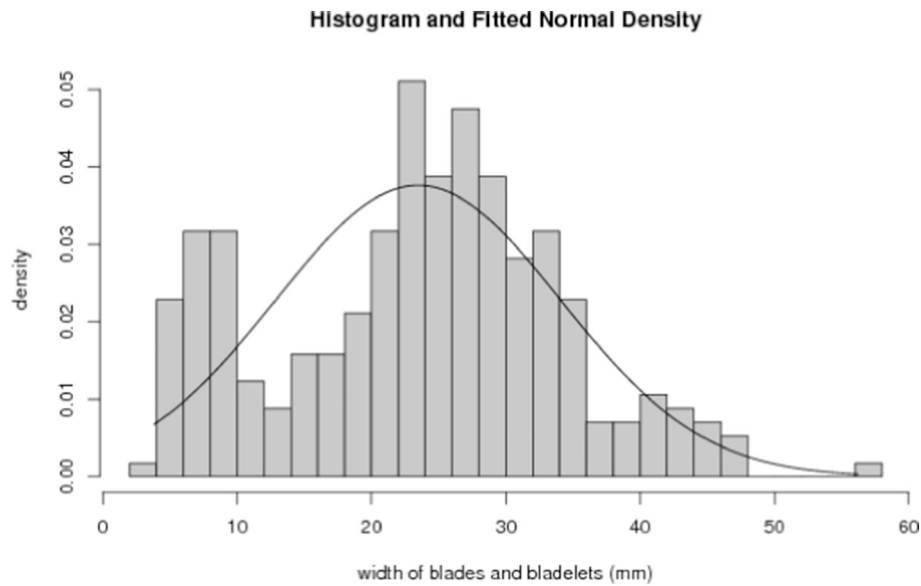


Fig. 9. Histogram showing the bimodal distribution of width (mm) of blades and bladelets. All assemblages are included ($n = 284$; 58 bladelets, 226 blades).

scars. Another platform core from BOS is pyramidal in shape with a convergent scar pattern. The product negative scars of type I cores are elongated and have either a blade or point shape (Figs. 15 and 22). The orientation of dorsal negatives of blanks supports a dominant unidirectional reduction (Table 8).

3.6.2. Types II and III: parallel regular cores

Parallel cores type II are rare with only two pieces found in BOS. Type III parallel cores are more numerous with two pieces in SMONE, three in BOS. The flatter core types II and III resemble parallel or Levallois-like cores. Most of these cores are flat in shape with a domed reduction surface, as typical for the Levallois method. The lateral convexity is frequently created by the production of debordants. Two of the cores have a convex lateral side created by a split cobble surface showing crushing and radiating marks from the point of impact ($n = 1$ in SMONE and $n = 1$ in BOS). This natural convexity of the core was used throughout the reduction, as even some cores in a relatively reduced stage still carry these distinctive marks (Fig. 6). The parallel cores can be divided into unidirectional parallel cores without an opposed platform, type II ($n = 2$, Table 11, Fig. 16), and distally prepared

parallel cores with a second platform, type III ($n = 5$, Fig. 17). This distinction is made because different product shapes are possible for type III cores (see Fig. 22). The types II and III cores are mostly elongated and display mostly blade and pointed blade negatives.

3.6.3. Types IV and V: parallel cores with irregular scar pattern

Type IV parallel cores occur, with two pieces in SMONE and five cores in BOS (Fig. 18). They show dominantly unidirectional removals, whereas type V ($n = 4$) indicates a bidirectional reduction of end products (Table 12, Fig. 22). Type V cores are only present in BOS with four pieces (Fig. 19).

Both types have an irregular negative scar pattern indicating the removal of mostly flake sized products. Types IV and V show relatively shorter reduction surfaces, compared to types I–III. The negative scars on the cores are irregular in shape, including those indicating the removal of triangular flakes. The type V cores are comparable to type IV but have a second equally used platform. They are generally much reduced and have more inclined platform angles than any of the other core types.

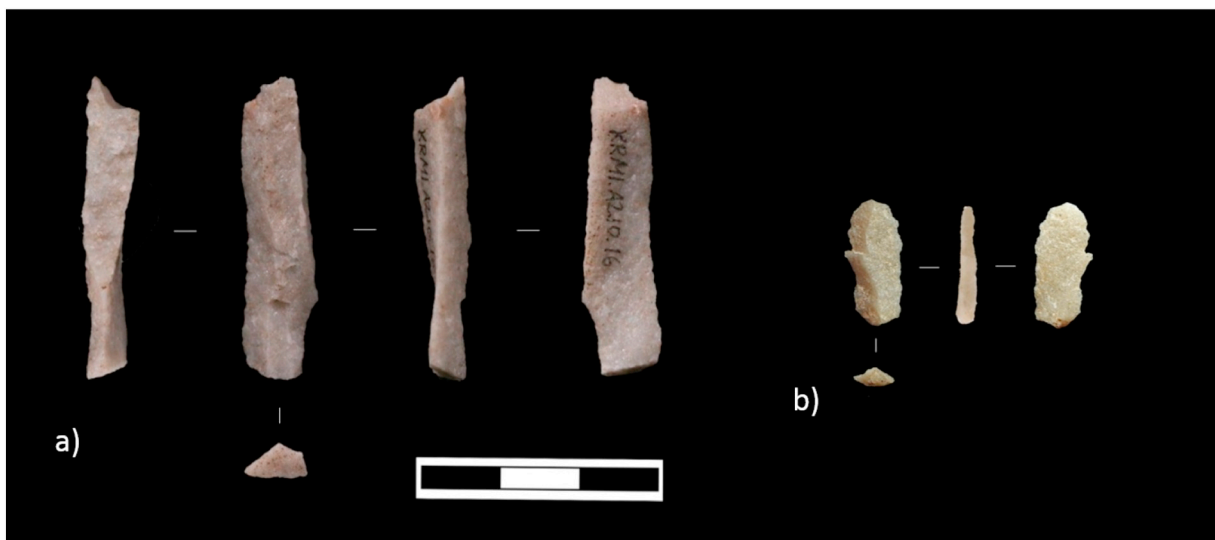


Fig. 10. Bladelets. a) #10.16, medium grain quartzite, SMONE; b) #C1.4, medium grain quartzite, SMONE.

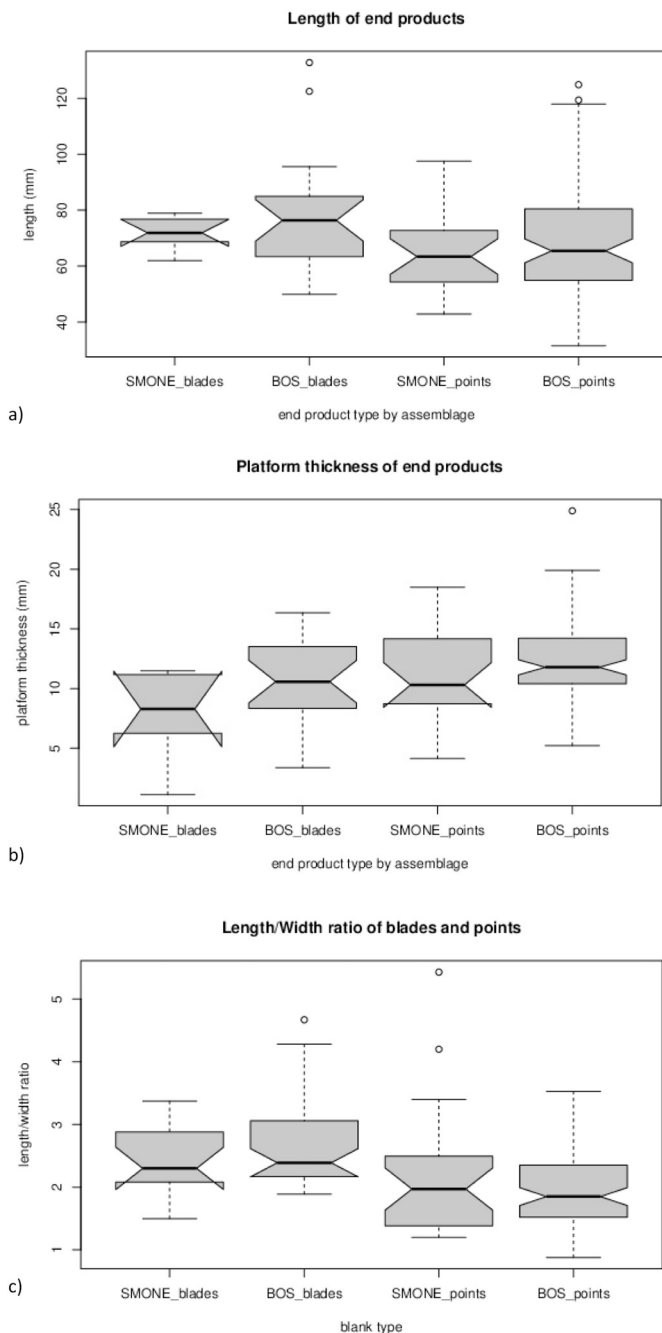


Fig. 11. Notched boxplot charts of a) length b) platform thickness and c) length/width ratio of blade and point end products in the different assemblages. (SMONE blades $n = 7$, points $n = 21$; BOS blades $n = 21$, points $n = 91$).

3.6.4. Bladelet cores

There is a persistent if small presence of bladelets in the assemblages (Table 2). There are a number ($n = 4$) of cores with bladelet scars (Fig. 20). The core blanks of the are chosen randomly, including one flake as blank, an exhausted core and two chunks. These cores have only been identified in BOS. The bladelet cores have a platform that is steeply angled to the production surface similar to those first described by de Sonneville-Bordes and Perrot (1954, p. 332) as carinated scrapers. The production surfaces of these cores are narrow, with 2–3 bladelet negatives directly adjacent or overprinting each other. One of the bladelet cores is created on a sizeable preparational flake with bladelet removals around a convex edge. This piece could be interpreted as a tool rather than a core, or even only as preparation of the dorsal edge.

The specimen do not show any preparation or other characteristics, than bladelet negatives, however, it is interesting that bladelet production systems are frequently described for the Howiesons Poort (Wurz, 2000; Villa et al., 2005; Soriano et al., 2007, Soriano et al., 2015). The bladelets and bladelet cores found at KRM in the MSA II lower could indicate that this strategy of bladelet production has deeper roots in the South African MSA than formerly thought.

3.6.5. Other core types

Tested cores ($n = 11$) with only one or two removals are quite numerous. Some of these are on flakes and produced elongated products (e.g. two large cores on flakes in BOS). Others could be described as informal platform cores, as the cobble blank is reduced using one platform, e.g. four cores in BOS, two of which are made on quartz cobbles (Table 5). There are also several exhausted multidirectional cores or those in which the direction of removals is not clear ($n = 7$). All the cores in altered quartzite ($n = 4$) have such disintegrated surfaces that they are not possible to characterize further. Two cores on coarse Table Mountain Sandstone are indeterminate. Four cores are recycled, and the second generation of reduction is only an informal or opportunistic flake production (Fig. 21). This is only seen in BOS where, after the production of elongated blades and points, an informal opportunistic flake production can be observed on a number of cores. Two of these are on regular platform cores and in the other cases, the original core systematic is not clear. Additionally, there are also several core fragments ($n = 10$, 15%).

3.6.6. Summary of cores

It is hypothesized that most of the informative cores are part of one main reduction system. This system mainly includes unidirectional cores (55% of the SMONE cores and 24% of the BOS cores). Bidirectional cores are only seen in BOS and in a small amount (7%). The bladelet cores are also reduced unidirectionally but do not show any of the morphologies typical on the other core types. Bladelet cores are only found in the lower BOS assemblage, although bladelets occur throughout the analysed layers. Some cores have been systematically exploited and then a second generation of three or more small flakes have been removed opportunistically (Fig. 21). As mentioned above, this recycling of cores is only seen in BOS ($n = 4$). The reworking of cores into tools is another phenomenon seen on three pieces in BOS, as discussed above. This observed recycling of cores in the BOS layer into second generation cores and the transformation into heavy duty tools can be seen as a separate step of the *chaîne opératoire*.

3.7. Synthesis

Most of the informative cores follow a unidirectional prepared core system (Fig. 22, I–IV) that can be seen on 19 cores (19/65). In SMONE six cores and in BOS 13 cores belong to the unidirectional reduction system. In BOS, there is also a low amount of cores attesting a real bidirectional reduction with two opposed equally-used platforms. All of these cores show remaining cobble cortex on the non-active part, which is the back or undersurface of the core (see Table 10 for core blanks). For the terms “undersurface” and “back” see, e.g. Wurz (2002, p. 1004) and Soriano et al. (2007, p. 686). These cores can all be classified into platform and parallel cores (Tables 11 and 12). The platform cores (type I) relate to a semi-rotational reduction system on pyramidal or prismatic cores. The parallel cores (types II–V) conform to a Levallois-like system with products removed parallel to the intersecting plane between the reduction surface and undersurface (Conard et al., 2004). The relationship between the cores is inferred on from the characteristics of the core and end product morphologies, as no complete or incomplete core reduction could be refitted. Core types I–III carry elongated scar patterns that are regular in size and shape; type IV and V cores have flake sized negative scars, which are irregular in shape. Type V cores are not represented in SMONE. With this core typology in mind,

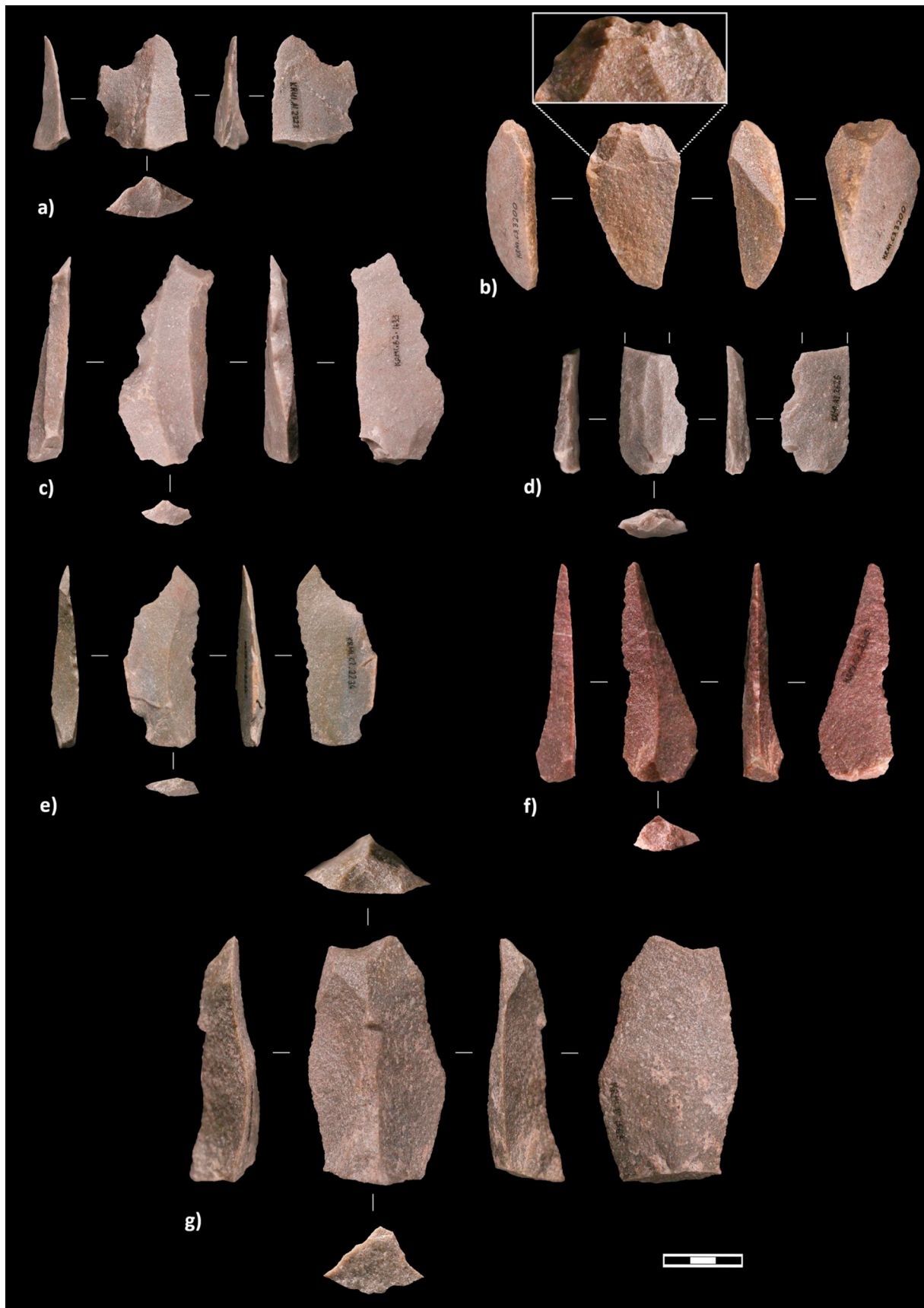


Fig. 12. Formal tools. All on medium grain quartzite; a) notched flake #2323, BOS; b) ventral scraper on thick debordant #3200, BOS (close up of retouch); c) denticulated blade #1633, BOS; d) notched blade fragment #2625, BOS; e) denticulated point #2234, BOS; f) lateral retouch on point #2340, BOS; g) distal notch on blade #1563, BOS.

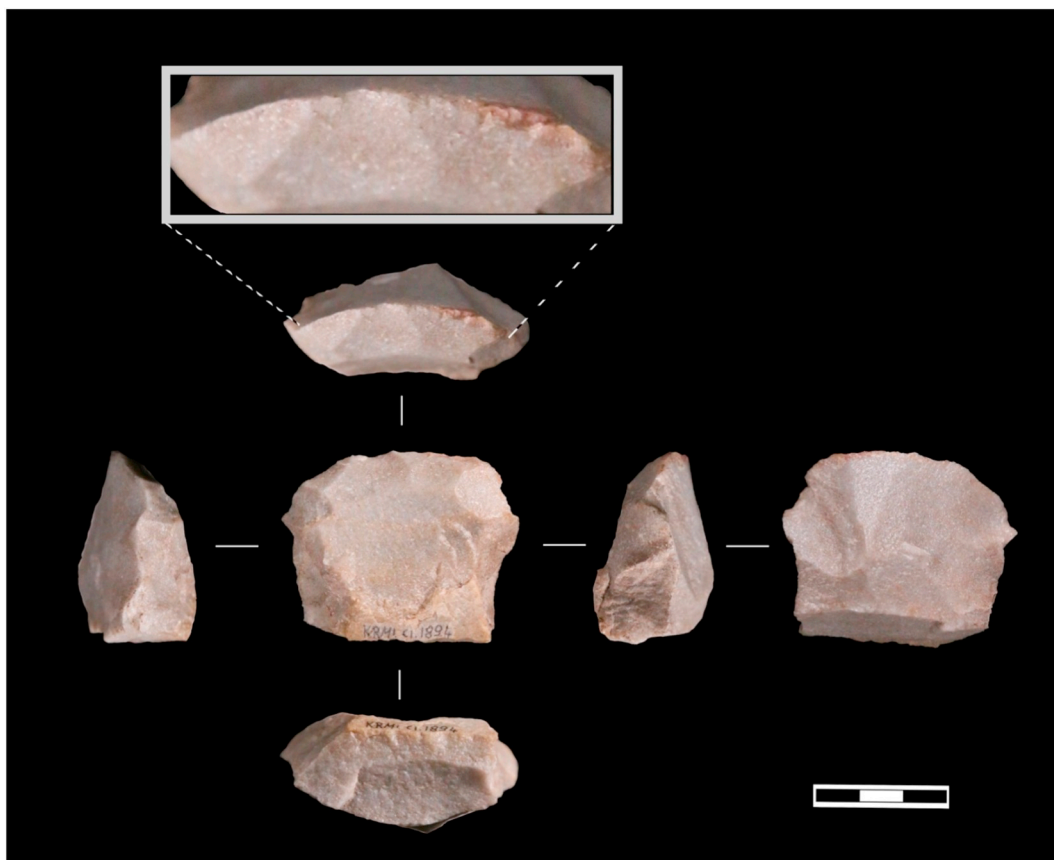


Fig. 13. Scraper on core. #1894, medium grain quartzite, BOS.

it is to mention however, that the differentiation between platform (type I) and parallel (types II–V) cores can be ambiguous, especially if a Levallois core geometry is combined with a semi-rotational (“around a corner”) production surface (cf [Conard, 2012](#), p. 245).

The described end product shapes can relate to different core types so that one shape can be produced by multiple core types. The blades are usually regular to very regular ([Damlien, 2015](#)) in their shape and negative scar pattern. They are most probably produced by types I to III cores ([Fig. 22](#)). Type 1 triangular pieces could be produced on any of the core types, but are, together with flakes, the main products of types IV and V cores, which only show flake sized negatives ([Fig. 22](#)). The broad variety of shapes (symmetric, asymmetric, skewed) of type 1 points can be explained by the irregular scar pattern of types IV and V cores. The type 1 points are most prevalent in BOS, and this assemblage also shows a higher amount of types IV and V cores ([Table 11](#)). Type 2 points can be correlated to core types I and II, platform and parallel cores, with a unidirectional reduction of regular elongated products ([Fig. 22](#)). This type is most common in SMONE. Type 3 is most likely produced by type III cores, which show a predominantly unidirectional reduction of regular elongated products but have distal preparation, necessary to create distal convexity to produce the pointed tip of the blanks. Flakes could be produced on any core type, but cores IV and V can only produce flake sized products. A bidirectional dorsal scar pattern is seen more often in BOS, which is in accordance with the frequency of bidirectional type V cores, which only appear in BOS (compare [Table 11](#)). However, types III and IV cores could also account for some of the pieces, as distal core preparation could infer a bidirectional scar pattern.

It is possible that when the platform cores type I were reduced in thickness, they transformed into parallel cores types II and III. As platform preparation and distal preparation continued, the parallel cores become shorter, resulting in cores types IV and V. Types IV and V

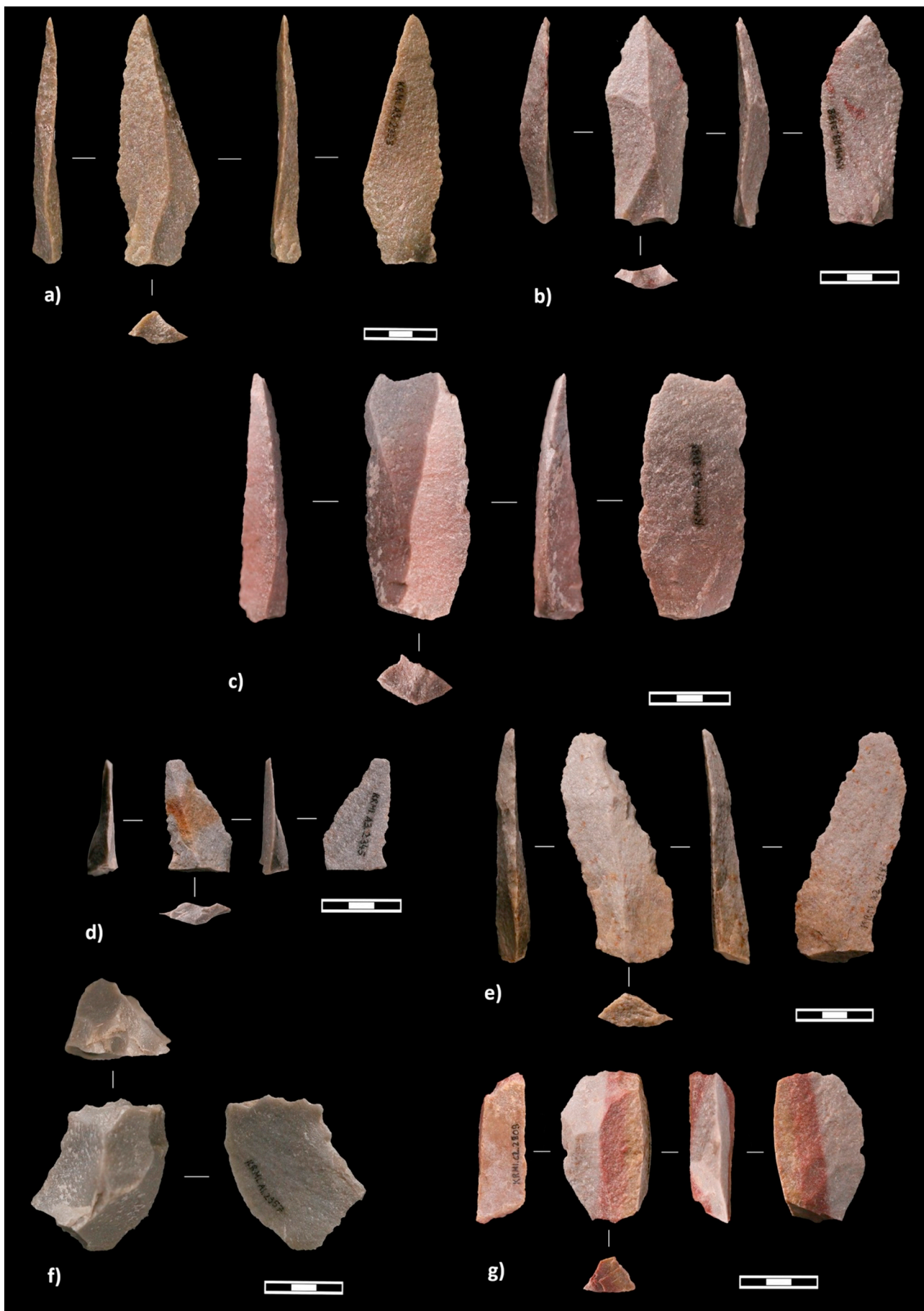
cores possibly represent the last stages of the reduction system.

As the classification of cores into the presented types is fluid and based on the variety of end product shapes, the reduction is proposed to be a single related system with the aim of producing multiple end-product morphologies, including different point shapes, blades and flakes. Similar systems of “combined manufacture” have been described by [Shimelmitz and Kuhn \(2018, p. 7\)](#) for a recurrent Levallois system.

4. Comparison to MIS 5 sites from the southern Cape

The results of the new analysis of the KRM material are discussed here in the context of the broader MIS 5 southern Cape landscape. Other sites from the southern Cape, which are compared here, are Cape St. Blaize ([Goodwin and Malan, 1935; Thompson and Marean, 2008](#)), Pinnacle Point 13B ([Thompson et al., 2010](#)) and 5–6 ([Brown, 2011](#)) and Blombos ([Douze et al., 2015](#)) ([Table A.10](#)).

The Pinnacle Point sites are located on the southern coast of the Western Cape, very close to the shore. Its proximity to Klasies River and the well-dated MIS 5 assemblages make it a priority candidate for comparison. **Pinnacle Point 13B** (PP 13B) contains two large MIS 5c (OSL dating 94 ± 3 ka to 124 ± 5 ka) assemblages, each comprising more than a thousand artefacts > 10 mm ([Thompson et al., 2010](#)). They stem from different sections of the site (an Eastern and a Western area), which are not correlated. A small collection of MIS 5d (OSL dating 110 ± 4 ka) ($n = 47$) is from the Lower Roof Spall from the Eastern area, and the MIS 5e (OSL dating 125 ± 5 ka) assemblage ($n = 255$) is from the LC-MSA Northeastern section. In the technological analysis by [Thompson et al. \(2010\)](#) the term “detached pieces” is used in the sense of blanks in this paper; “end products” in Thompson include all points, blades and Levallois flakes, including debordants. Cores are described by a different typology, which mixes different approaches ([Thompson et al., 2010](#)), complicating inter-site comparisons. Based on the



(caption on next page)

Fig. 14. Edge damage. All on medium grain quartzite; a) damage on point #2353, BOS; b) damage on point #3138, BOS; c) damage on blade #3181, BOS; d) damage on point #2345, BOS; e) damage on blade #2185, BOS; f) scraper damage on flake #2957, BOS; g) scraper damage on flake debordant #2809, BOS.

platform and parallel core descriptions and drawings, a dominantly unidirectional reduction system for points (converging scar pattern) and blades (parallel scar pattern) can be deduced. There is also a high amount of “prepared cores” with a centripetal pattern.

The most apparent similarities between the PP 13B and KRM assemblages is the use of quartzite as primary raw material, with 83% at PP 13B and 80.4–90.8% at KRM. Cobble cortex is visible on 17.5% from all artefacts from PP 13B compared to 28.4–38.7% at KRM. [Thompson et al. \(2010, p. 262\)](#) use the term “point” in the sense of convergent flake-blades, referring to [Goodwin and van Riet Lowe \(1929\)](#), although they also include asymmetrical pieces. The Pinnacle Point 13B points therefore either fit into the type 1 or 2 point category described for KRM. The proportion of blades to points at PP 13B shows mostly a higher amount of blades, except in the Western MIS 5c assemblage where points are a bit more frequent (10.9% of blanks on average). It is apparent, that the proportion of bladelet production is much lower at PP 13B than at KRM, but a minor bladelet component is evident. In contrast to the KRM assemblages discussed here, the blades and bladelets are described as having a uni-modal width distribution, which does not point towards a separate reduction sequence for the bladelets ([Thompson et al., 2010](#)). The formal and informal tool component at PP 13B is amalgamated but still shows very low numbers with an average proportion of 2% in relation to all debitage (no size cut-off, as opposed to KRM where the assemblage composition is analysed in relation to pieces > 20 mm).

The lithic material of **Pinnacle Point 5–6** (PP 5–6) was examined by [Brown \(2011\)](#). The early assemblages dating to MIS 5 b-a (OSL dating 86 ± 3 ka to 79 ± 3 ka) are so far only described in his PhD thesis. They belong to the LBSR stratigraphic unit and are subdivided into six occupational horizons. The uppermost occupation layer is called Jed/JR Quartzite and contains 925 lithic artefacts (there is no size cut-off). The other assemblages of LBSR only include less than a hundred lithic artefacts, which is why they are not included here ([Brown, 2011](#)). The main raw material is quartzite, and a high amount of artefacts show remaining cobble cortex. There are only seven cores, and most of them have been opportunistically exploited so that the systematic reduction is no longer visible. Three cores are attributed “single platform cores” (the terms are based on [Volman \(1978\)](#)) which are described by [Brown \(2011\)](#) as fitting the point-core definition of [Wurz \(2000\)](#). The blanks show dominantly unidirectional parallel and convergent dorsal scar patterns. Most end products are points (63%), followed by blades (37%), no flakes have been identified as such. Furthermore, there is a number ($n = 14$) of cortical debordants, which accounts for maintenance of lateral core convexity. 33% of the end products have a prepared faceted platform. The hypothesis is that the reduction system was mainly unidirectional ([Brown, 2011](#)). According to [Brown \(2011\)](#), there is only an informal tool component in the MIS 5 assemblages of PP 5-6.

The **Cape St. Blaize Cave** (CSB) is situated at the coast in the town of Mossel Bay. The MSA material was first described by [Goodwin and Malan \(Goodwin, 1930; Goodwin and Malan, 1935\)](#) in the 1930s. A more recent re-evaluation of the lithic material by [Thompson and Marean \(2008\)](#) produced different results compared to the initial analysis. As none of the papers defines what is meant by points (e.g. if blade dimensions are included, or if it is only for symmetrical flakes), the data of both analyses are given with [Goodwin and Malan's](#) data in brackets ([Table A.10](#)). It needs to be kept in mind that the excavations took place at an earlier time and there might be a sampling bias towards tools and

complete artefacts, which could explain the very high percentages for retouched pieces and faceted platforms. Neither [Goodwin and Malan \(Goodwin, 1930; Goodwin and Malan, 1935\)](#) nor [Thompson and Marean \(2008\)](#) analysed the assemblages in relation to reduction sequences, therefore only attribute data of cores and blanks can be presented here.

The raw materials are all from local primary and secondary sources. It is the first assemblage that has been attributed to the Mossel Bay techno-complex ([Goodwin, 1930](#)), which is characterized by a high amount of points and blades which are reduced in a Levallois-like system. [Thompson and Marean \(2008\)](#) describe the cores as radial cores, as well as blade and point cores. Contradictory to the previous studies, [Thompson and Marean \(2008\)](#) describe the frequency of blades higher than that of points, and flakes being the dominant blank type. Platform faceting is very common, with over 50%. The formal tools are mostly denticulates, notched pieces and retouched points. The described assemblages of KRM are characterized as belonging to the Mossel Bay techno-complex. However, the vague definition based on the CSB material makes a clear association difficult, as mentioned by [Thompson and Marean \(2008\)](#).

Blombos Cave (BBC) is situated on the south coast of the Western Cape. The material of the M3 phase is described in [Douze et al. \(2015\)](#) and dates to MIS 5 c-b (OSL and U/Th dating 101 ± 4 ka to 94 ± 3 ka ([Tribolo et al., 2006; Douze et al., 2015](#)). Like KRM, BBC is situated very close to beaches and rivers. The raw materials in the form of cobbles all stem from these local sources. However, the main raw material used is silcrete from secondary marine sources; quartzite and quartz only represent a minor component in the assemblage. The BBC lithic artefacts of the M3 phase comprise 3404 pieces > 2 cm ([Douze et al., 2015](#)). The reduction technique in both sites BBC and KRM is freehand percussion with a hard hammer ([Douze et al., 2015](#)). The main debitage products at BBC are triangular flakes encompassing 20% of all complete debitage. The triangular flakes exhibit more faceted (27%) and dihedral (27%) platforms than other blank shapes. The same pattern is seen at KRM, where points more often show faceted platforms ([Table 6: 37.5% and 45.5% of faceted pieces are points in SMONE and BOS, respectively](#)). Dihedral platforms, however, are scarce at KRM. The triangular flake end products at BBC are attributed to different reduction systems, and as described for KRM, the shapes between triangular flakes vary significantly especially in the broadness of the base and in their length. Three main triangular point morphologies are identified at BBC in the M3 phase. *Déjeté* points, which are axially asymmetrical, have short and large bases and thick plain or dihedral platforms, are related to discoid/inclined reduction methods, but also to parallel centripetal or unidirectional methods. At KRM no *déjeté* points occur. At BBC the second category of elongated thinner triangular flakes exists. They are axially more symmetrical points with Levallois points representing the most standardised within this class. These are linked to parallel unidirectional reduction, including parallel/Levallois-type methods. At KRM some types 1 and 2 points resemble these Levallois triangular flakes, and it is surmised that they have been produced using a similar parallel unidirectional method. The third type at BBC comprises triangular blanks originating from core maintenance and preparation phases and they are very variable in shape. At KRM there also triangular blanks from preparational phases, but they are not included in the end product morphologies.

At KRM it is proposed, that a combined manufacture of multiple end product shapes existed in one core reduction system. For this reason, we

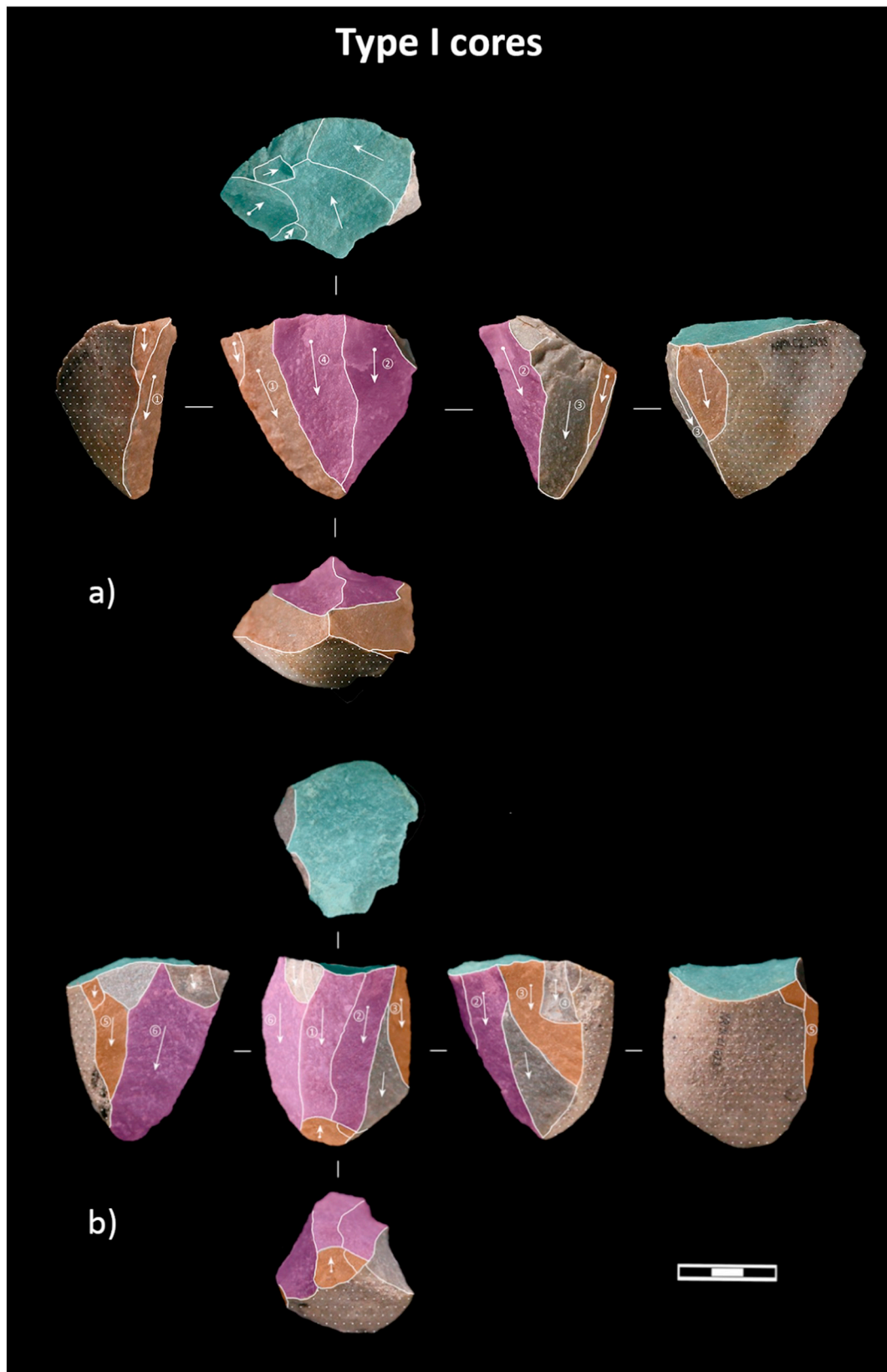


Fig. 15. Cores type I. a) #3255 medium grain quartzite, BOS; b) #1623, medium grain quartzite, BOS. In Figs. 15–21 the cores are colour coded with pink indicating the production surface, preparational negatives are marked in orange, and the core platform is coloured in blue. Cortex is indicated with a dotted surface. The arrows indicate the direction of removal. The numbers in circles are the result of the diacritic reading and show the possible order of the removals.

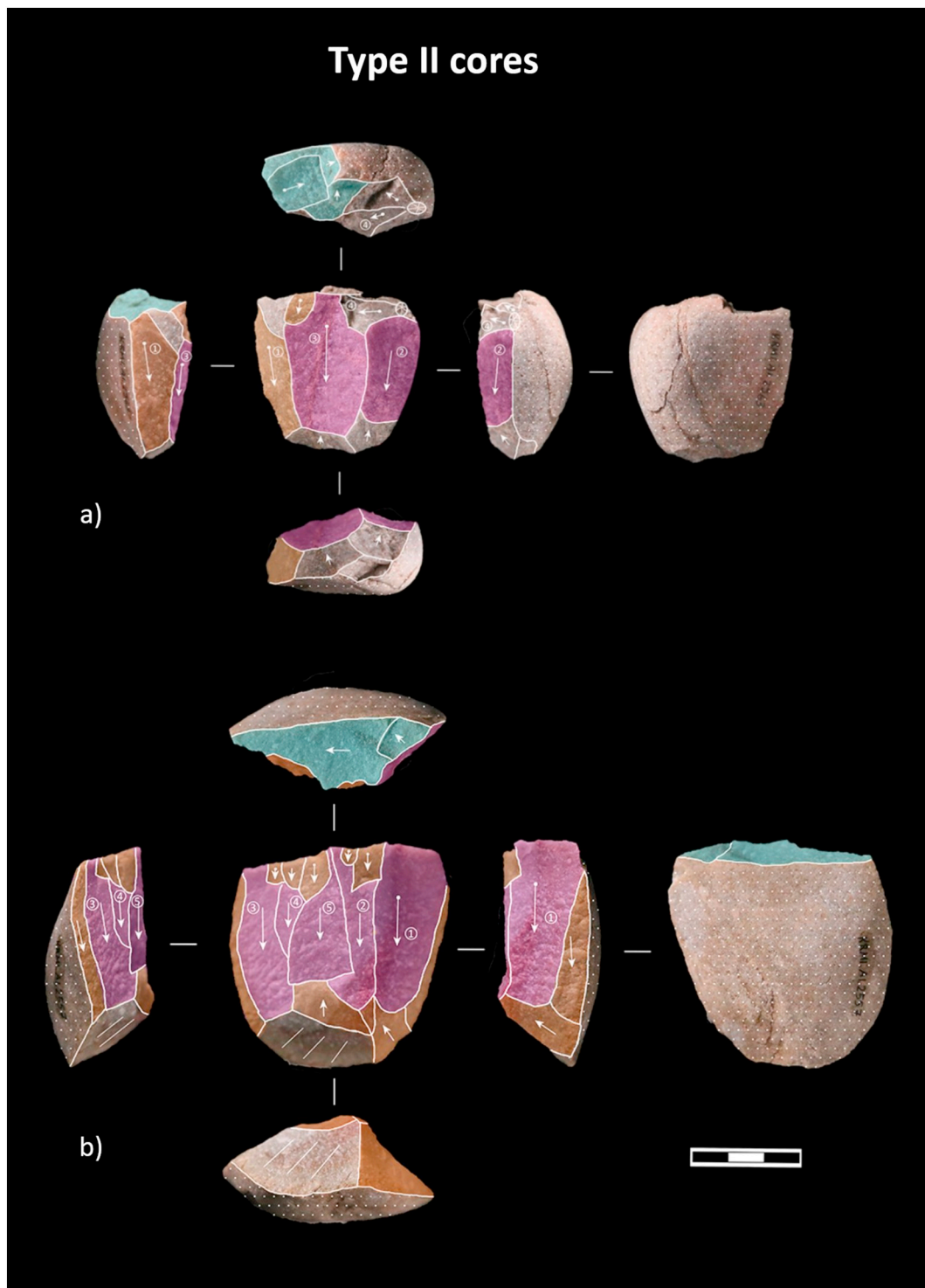


Fig. 16. Core type II. a) #2967, medium grain quartzite, BOS; b) #2556, medium grain quartzite, BOS.

established a new taxonomy of end product morphology to do justice to the high variability, which includes shapes different point types, blades and flakes.

The unidirectional and unidirectional convergent cores described by Douze et al. (2015, p. 13) are comparable to the KRM cores of types II, III and IV, which are also parallel and mostly unidirectional. One

bidirectional-opposed core that follows the same system as the other parallel cores is also described (Douze et al., 2015, p. 13), which is similar to the type V cores seen at KRM. The reduction method is therefore quite similar between BBC and KRM. However, KRM shows more variability in the core morphology in the unidirectional system and exhibits more bidirectional reduction. Furthermore, BBC shows

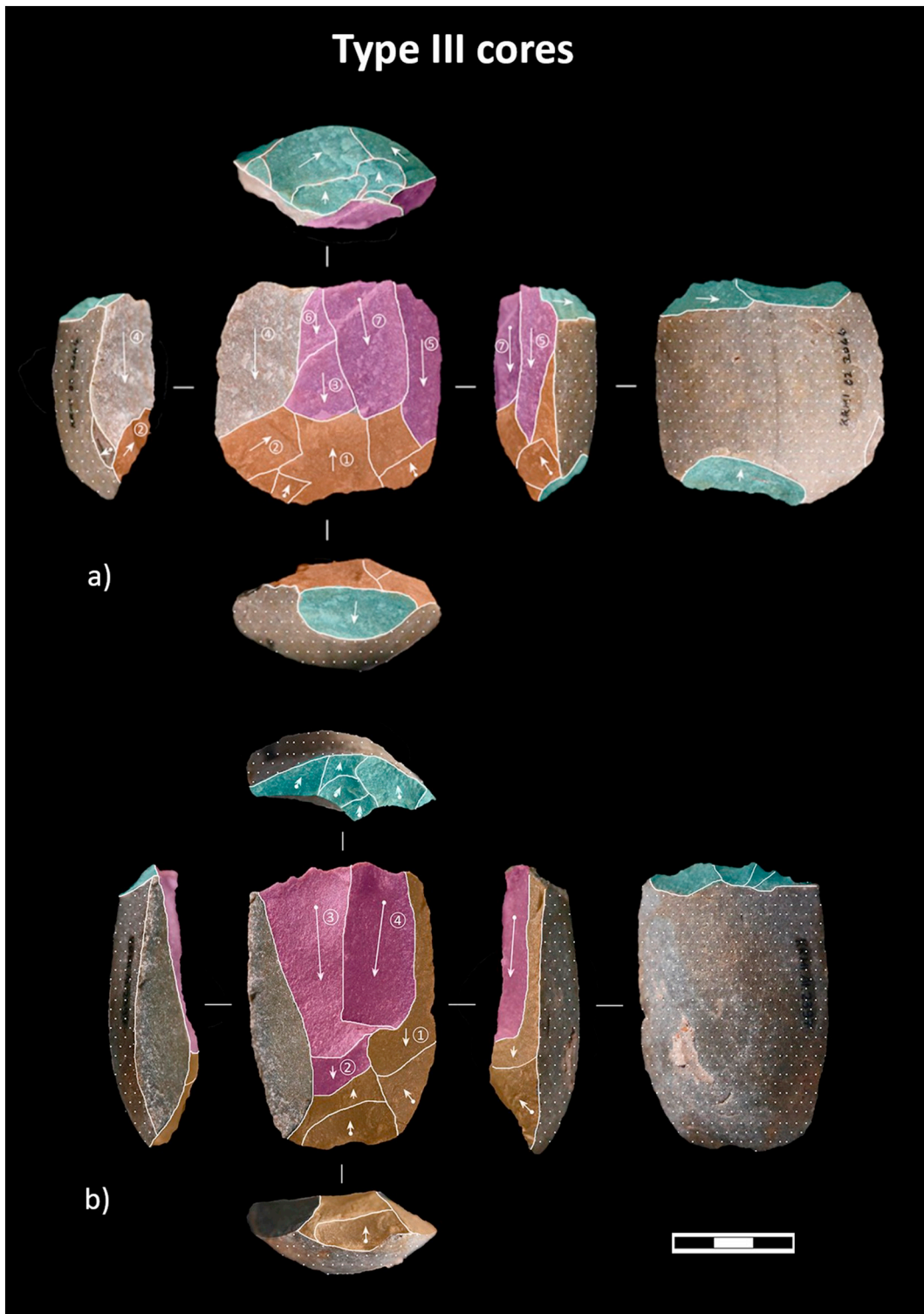


Fig. 17. Core type III. a) #2044, medium grain quartzite, BOS; b) #2397, medium grain quartzite, BOS.



Fig. 18. Core type IV. a) #3241, medium grain quartzite, BOS; b) #1405, medium grain quartzite, BOS.

other reduction systems, like inclined and centripetal reduction, which is absent at KRM.

The blade-sized pieces (2:1 ratio) at BBC make up 8% of complete blanks; they are not distinguished into pointed or other shape. At KRM the blades comprise 6.9% in SMONE and 12.9% in BOS. However, blade sized points occur with frequencies of 6.8% in SMONE and 7.5% in

BOS, so the material of KRM shows more elongated pieces than that of BBC. Although blades are produced at BBC, the unidirectional cores are all shorter than wide, only showing flake sized negatives. The lateral convexities are established by common reduction of debordants (9.1% of blanks). The blanks show frequent platform preparation with faceting (15.7%), although the points are more often faceted (27%); the

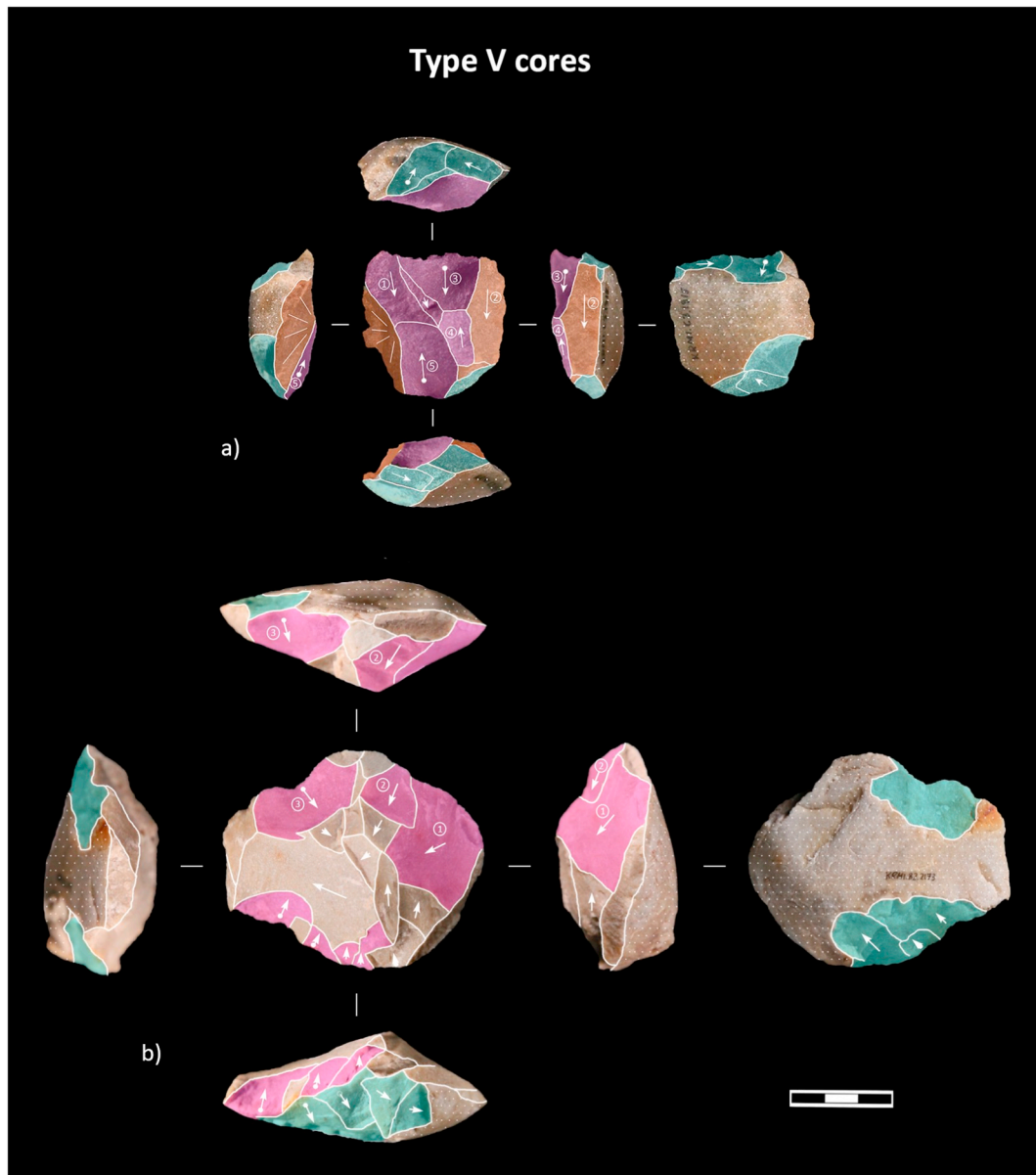


Fig. 19. Core type V. a) #1915, medium grain quartzite, BOS; b) #2173, medium grain quartzite, BOS.

same pattern is seen at KRM (Table 6: 37.5% and 45.5% of faceted pieces are points in SMONE and BOS respectively).

Similar to KRM, the frequency of formal tools is low with 2.3% at BBC. Unlike KRM, the proportion of edge modification by damage and use wear is low in the BBC assemblage (1.5%) as opposed to KRM where it is 16.4% in SMONE and 21.7% in BOS. Nevertheless, unmodified blanks are also interpreted to be used as tools (Douze et al., 2015, p. 6).

4.1. Common trends and variability between MIS 5 assemblages

The similarities between sites on the southern Cape have been referred to before (Wurz, 2013; Mackay et al., 2014; Douze et al., 2015). Typical characteristics are the dominant use of local raw materials, a direct hard hammer internal percussion technique, a low frequency of

formal tools with denticulates and notches prevailing and common platform faceting. Local raw materials comprise about 90–100% in all assemblages; the rock type can differ between available sources of quartzite and silcrete. The presented MIS 5 assemblages a direct internal percussion with a hard hammer is described, e.g. by the presence of common *siret* fractures and hammer stones. The amount of tools is commonly very low in MIS 5. Most assemblages have tool frequencies around 2%. Nevertheless, PP13B MIS 5c West exhibits 4% tools and the most extensive tool component (12.8%) is found in CSB (following Thompson and Marean, 2008). However, as mentioned above, CSB is most probably affected by collection bias so that tools might be over-represented. Another similarity between the presented assemblages is a frequent faceting of platforms. The frequency varies from 15% up to 52%.

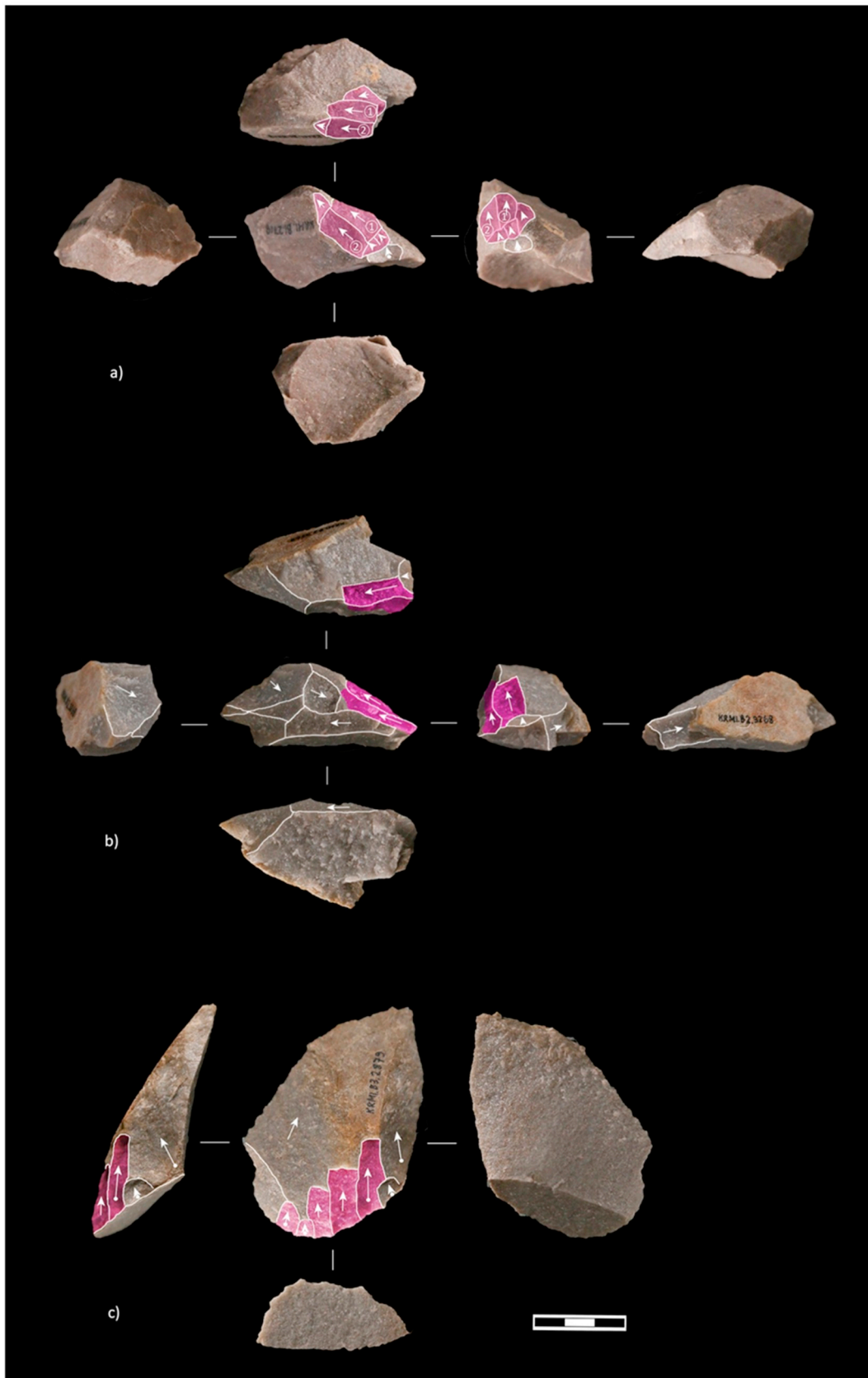


Fig. 20. Bladelet cores of BOS. All on medium grain quartzite; a) #2718, BOS, core on chunk; b) #3268, BOS, core on flake fragment or chunk; c) #2879, BOS, possible core on flake.

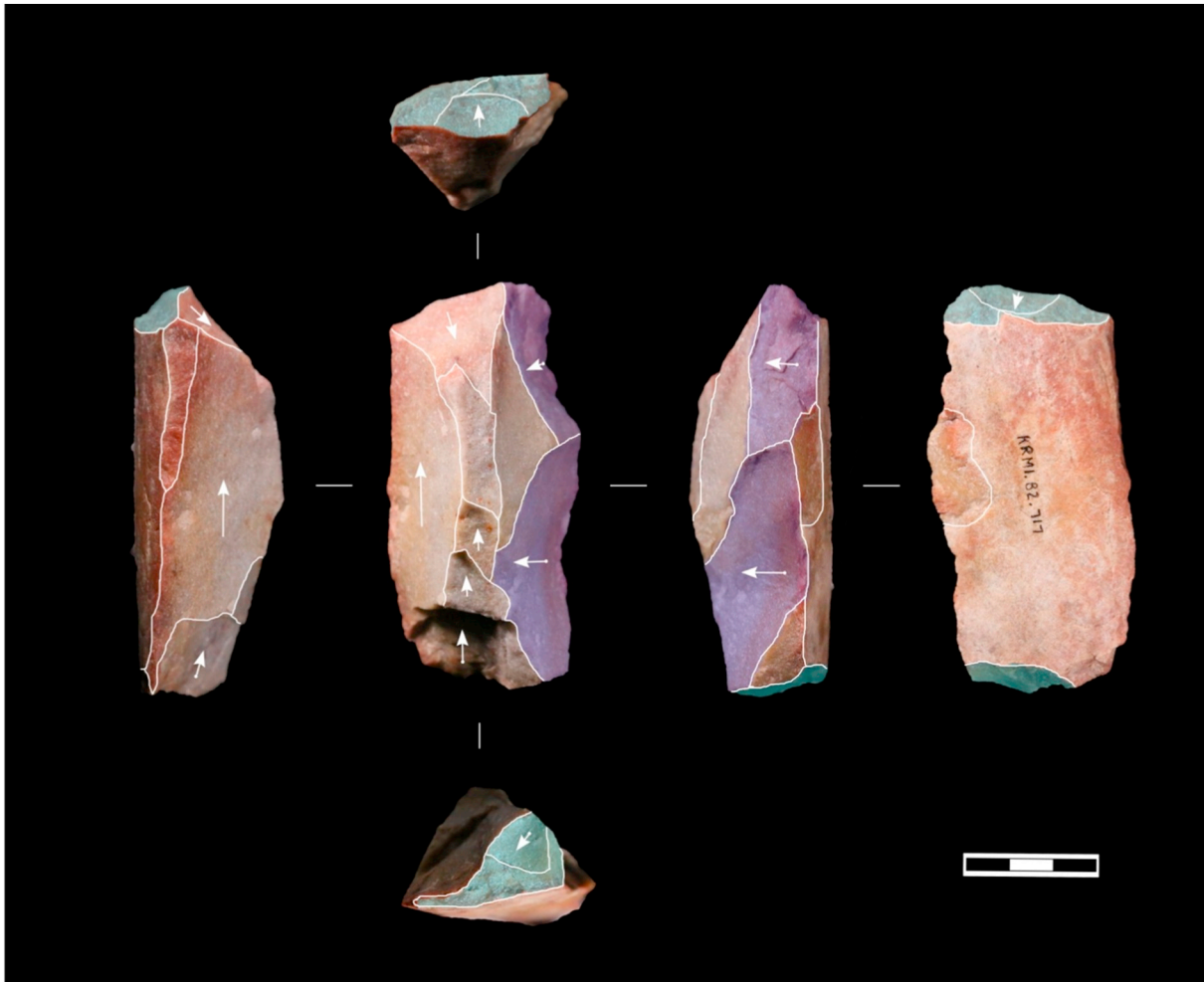


Fig. 21. Core #717 of BOS (on medium grain quartzite) with secondary orthogonal informal flakes in purple overprinting a systematic reduction (opposed platforms of first generation core in blue).

Differences in technology are seen in reduction sequences and the shape of end products. As for reduction systems, a unidirectional reduction is seen at all sites, however additional co-existing reduction systems differ. The described unidirectional reduction systems are on parallel and platform cores. At KRM a complementary bidirectional reduction is seen, whereas the other sites mostly display a centripetal reduction (Levallois and inclined). The reduction systems allow for some differentiation, which can be further defined by the blank morphologies. Point and blade production seem to differ in frequency. Dominant blade production is only seen at CSB (following [Thompson and Marean \(2008\)](#)). More focus on the point production is seen at BBC, KRM and PP5-6. The PP13B assemblages show an equal production of both points and blades.

This attests, that although MIS 5 technology on the southern Cape show many similarities, variation exists in the reduction systems which leads to different frequencies of end product shapes. A more detailed comparison of short term developments combined with refined dating at each site could reveal possible further relatedness or variety.

5. Discussion

Both KRM assemblages discussed here share characteristics with the MSA II or Mossel Bay techno-complex, previously described by Wurz (2000; 2002). One main reduction system is found in the assemblages discussed here, a unidirectional parallel system for the production of mainly points, but also blades. This fits as well with the description of Wurz's analysis of the larger MSA II assemblage at KRM. Additionally, a bidirectional parallel reduction is seen in one of the assemblages, BOS; and a bladelet component occurs in both assemblages, a phenomenon not previously described for the Klasies River MSA II assemblages. A more detailed degree of variability through time is furthermore evident in this analysis, due to the more refined focus used here. A summary of the comparison between the assemblages with the statistical values is provided in [Table A.9](#).

Technologically, SMONE exhibits a distinct character that differentiates it from BOS. SMONE has significantly fewer cores as confirmed by a chi-square test ($p < .05$). They seem to be smaller and lighter than in BOS (although only marginally significant, see [Table A.9](#)). SMONE also has a significantly richer flake component than BOS ($\chi^2(1) = 4.31$,

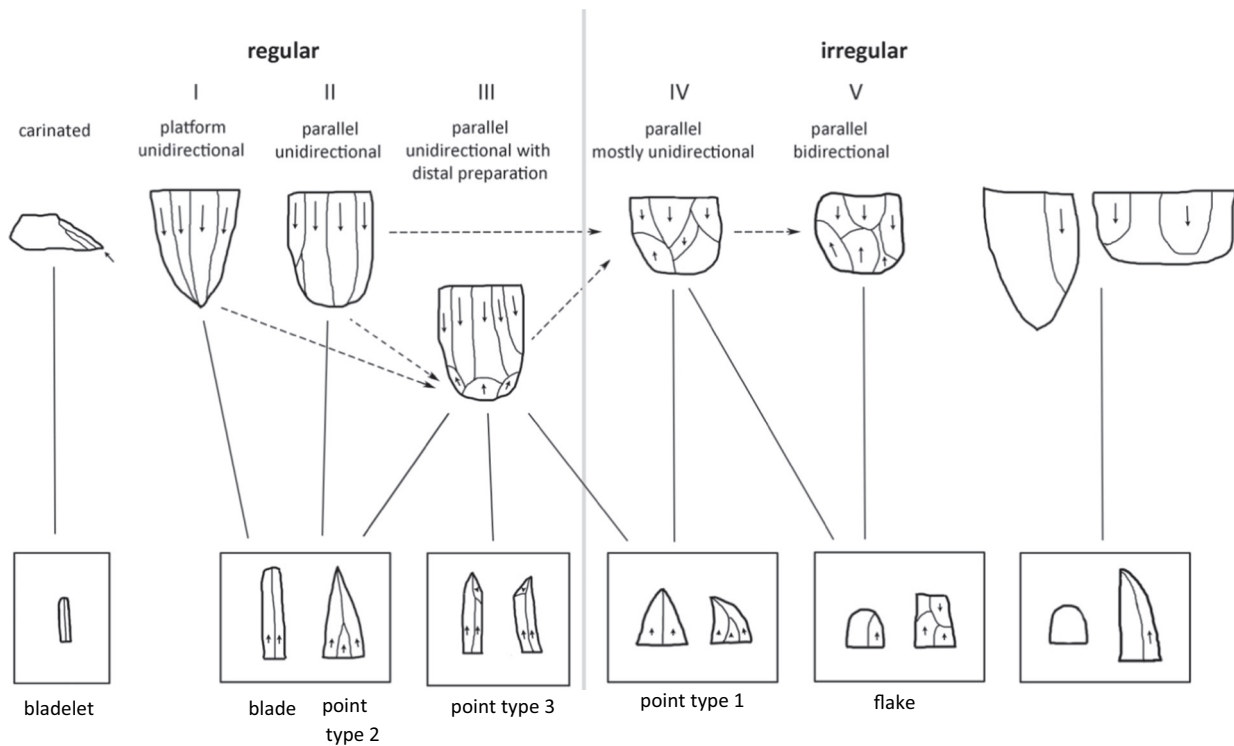


Fig. 22. Scheme of different core types with the corresponding product shapes. Core types are illustrated at the top, and end product shapes are at the bottom. The lines indicate which core types produced which types of end products. The cores are divided into types with a regular organization of negatives and those with irregular organization. The bladelet cores on the left are related to bladelet production. Core types I–V form the main reduction system. The main reduction system entails unidirectional prepared cores for the production of triangular flakes, elongated points and blades. (The pointed end products indicated in blue are, from the left, point types 2, 3 and 1; as discussed in more detail above). Apart from this, there are a few cores which are tested, indeterminate or with only a single product removed. They are grouped under “other”. The dotted arrows are hypothetical connections in the main core reduction system.

$p < .05$), although points and blades are more frequent in BOS (points: $\chi^2(1) = 7.16, p < .05$; blades $\chi^2(1) = 3.90, p < .05$). Bladelets also occur significantly more frequently in SMONE ($\chi^2(1) = 17.5, p < .05$), although they occur in the absence of bladelet cores.

Furthermore, the SMONE tool component is significantly smaller ($\chi^2(1) = 8.91, p < .05$) and less variable than in BOS, comprising only of denticulate and notches. No scrapers or lateral retouch have been observed, and the edge damage frequency is also half as frequent as in the BOS layers. The technological characteristics of the blanks and cores also differ between SMONE and BOS. Core types II and V are not present in SMONE. The end product platforms are significantly less

frequently faceted than in the BOS layer ($\chi^2(1) = 4.21, p < .05$). However, the blank platforms of SMONE show more informal faceting ($\chi^2(1) = 5.41, p < .05$). The external platform angle of the blades shows a significant difference between the layers attested by a Mann-Whitney U test ($U = 436, p < .05$). The products of BOS are heavier, especially the points ($U = 436, p < .05$).

These differences seen between SMONE and BOS justify their division into separate layers. Although we have shown, that statistically significant differences between the layers exists, the dorsal scar patterning on end products for all the assemblages shows predominately unidirectional patterns, and the dimensions of cores and end products

Table 5

Number and percentage of complete end products and the average of length (mm), width (mm), thickness (mm) and weight (g).

Measurement/end product	Complete end products		Length	Width	Thickness	Weight
	n	%	Average (mm)	Average (mm)	Average (mm)	Average (g)
Point						
SMONE	21	53%	66.4	32.7	12.1	21.7
BOS	92	68%	67.4	36.8	13.3	29.7
Blade						
SMONE	7	17%	72.3	27.5	11.6	24.0
BOS	21	14%	82.0	29.8	12.4	30.4
Flake						
SMONE	12	30%	49.3	33.8	11.2	17.8
BOS	19	18%	58.8	39.2	13.9	37.3

Table 6
Platform types of end products (n) with total values in per cent (%) (of proximally preserved pieces).

Platform type/ end product	Plain	Facetted	Informal facet	Dihedral	Cortical	Shattered	Total
Point							
SMONE	–	9	10	–	1	1	21
BOS	2	65	20	2	2	1	92
Blade							
SMONE	1	2	2	–	–	1	6
BOS	–	14	4	2	–	1	21
Flake							
SMONE	1	2	5	1	–	1	11
BOS	3	7	5	2	2	1	20
End product fragment							
SMONE	2	11	14	–	2	1	30
BOS	13	57	31	–	4	2	107
Total %							
SMONE	5.9%	35.3%	45.6%	1.5%	4.4%	5.9%	100% (n = 68)
BOS	7.5%	59.6%	25.0%	2.5%	3.3%	2.1%	100% (n = 240)

Table 7
Proximal preparation of the dorsal edge of the platform of end products (n) with total values in per cent (%) (of proximally preserved pieces).

Proximal preparation/ end product	None	Longer removals along scar ridges	Step flaking and trimming	Trimming and rubbing	Total
Point					
SMONE	10	5	6	–	21
BOS	49	11	29	3	92
Blade					
SMONE	4	1	1	–	6
BOS	11	2	8	–	21
Flake					
SMONE	5	–	6	–	11
BOS	10	2	8	–	20
Blank fragment					
SMONE	17	–	11	3	31
BOS	42	14	49	1	106
Total %					
SMONE	52.2%	8.7%	33.3%	4.3%	100% (n = 69)
BOS	46.9%	12.1%	39.3%	0.2%	100% (n = 239)

Table 8
Orientation of dorsal negative scars of complete end products.

Orientation of dorsal negatives	SMONE		BOS	
	n	%	n	%
Unidirectional convergent	3	8.3%	20	15.0%
Unidirectional parallel	3	8.3%	14	10.5%
Unidirectional	8	22.2%	23	17.3%
90° unidirectional	9	25.0%	15	11.3%
Uni- or bidirectional	6	16.7%	26	19.5%
Bidirectional	6	16.7%	31	23.3%
Orthogonal	–	–	2	1.5%
Multidirectional	–	–	1	0.8%
Indeterminate	1	2.8%	1	0.8%
Total	36	100%	133	100%

Table 9
Tool types. Amount (n) with percentages in relation to all pieces > 20 mm (%).

Tool type/assemblage	SMONE		BOS	
	n	%	n	%
Denticulate/notched piece	4	0.7%	15	1.2%
Point	2	0.4%	2	0.2%
Blade	–	–	4	0.3%
Flake	2	0.4%	10	0.8%
Scraper	0	–	8	0.6%
Point	–	–	1	0.1%
Blade	–	–	1	0.1%
Flake	–	–	1	0.1%
Core	–	–	4	0.3%
Combination notched/scraper	0	–	3	0.2%
Flake	–	–	3	0.2%
Lateral retouch	0	–	9	0.7%
Point	–	–	6	0.4%
Blade	–	–	1	0.1%
Flake	–	–	2	0.2%
Total formal tools	4	0.7%	35	2.8%
Edge damage	100	16.4%	270	21.7%
Point	24	3.9%	117	9.4%
Blade	24	3.9%	71	5.7%
Flake	22	3.6%	35	2.8%
Indet fragment	30	4.9%	47	3.8%
Total	104	17.1%	305	24.5%

Table 10
Core blank types (n) per layer.

Core blank	SMONE	BOS
Debordant	1	7
Flake	2	4
Cobble	6	35
Hammerstone	1	1
Indeterminate	1	7
Total	11	54

Table 11
Core types. Number and per cent by layer.

Core types	SMONE		BOS	
	n	%	n	%
Platform	2	18.2%	3	5.5%
Type I				
Parallel unidirectional				
Type II	–	0%	2	3.7%
Type III	2	18.2%	3	5.5%
Type IV	2	18.2%	5	9.3%
Parallel bidirectional				
Type V	–	0%	4	7.4%
Bladelet	–	0%	4	7.4%
Recycled	–	–	4	7.4%
Exhausted	1	9.1%	6	11.1%
Tested	2	18.2%	9	16.7%
Altered surface	–	–	4	7.4%
Indeterminate	–	–	2	29.7%
Fragment	2	18.2%	8	14.8%
Total	11	100%	54	100%

are similar. The same core reduction system is also seen in both layers. This justifies the classification into a common techno-complex, the MSA II.

All assemblages at KRM comprise an expedient (cf Binford, 1977; Kuhn, 1995, p. 26) technology. At KRM the expediency is evident by on-site manufacture, the use of local raw materials, no raw material selection for tool production, some cores are not completely exhausted, and the dominance of unretouched blanks. SMONE, however, may be described as more expedient than the BOS assemblage, as there are fewer tools and less investment in producing the artefacts, as evident in the lower degree of faceting of platforms. The lighter products in SMONE could relate to sorting and some rolling, as observed for the larger excavation of layer 17a by Singer and Wymer (1982). However, the technological differences, the lack of bidirectional exploitation and lesser preparation of the platforms are harder to explain through taphonomic factors. The recycling of cores and big flakes into second generation cores or tools in BOS can be seen as an indication of opportunistic utilisation.

These differences can also be interpreted in the context of provisioning systems (e.g. Kuhn, 1995; Mackay et al., 2018). Two distinct provisioning systems occur, provisioning of individuals and provisioning of place (Kuhn, 1995). Individual provisioning systems prepare mobile individuals for unreliable resource availability. Such toolkits for individual provisioning mostly include cores, from which tools can be manufactured as needed, and formal multi-purpose tools, which can be resharpened after use (Kuhn, 1995; Mackay et al., 2018).

A site relying on provisioning of place exhibits less evidence for mobility over long distances as evident in the absence of exotic raw materials and on-site production and discard of tools. On-site manufacture is visible by the presence of multiple cores and debitage recording different stages of the reduction sequence. Place provisioning is also characterized by prolonged or re-occurring occupations of a site and therefore, predictable resources close by (Kuhn, 1995; Mackay

et al., 2018). In the KRM assemblages discussed here, local raw materials are used and reduced on-site, as indicated by the presence of cobbles, cortical flakes, cores and small debitage. Some of the cores are discarded without being fully exhausted (e.g. the type I platform cores in Fig. 8). The end products show a high variety in size and shape. The use of unretouched blanks as tools and only a small amount of formal retouch shows minimal input into the production of tools. The formal tools indicate that tools were not resharpened or recycled after use, but discarded. Therefore it might be that tools were produced for a short life cycle and not with the intention of transport or the equipment of individuals, implying low mobility of the group. The scarcity of unretouched pieces in the South African early MSA is sometimes interpreted as a missing final phase of tool production following Geneste (1985), with only early and middle phase present (see, e.g. Goodwin and Malan, 1935; Marean et al., 2004, p. 48). In the case of KRM, however, the unretouched points have been used as tools, and the last phase is therefore not missing. Following Kuhn (1992, 1995) it is suggested that KRM during MIS 5 for the assemblages discussed here, functioned as a residential site with provisioning of place.

Regarding provisioning and mobility in the greater landscape, the southern Cape sites show similar patterns to KRM. As described above, the presented sites conform to most characteristics which imply provisioning of place behaviour at a residential site (following Kuhn (1995)). This could mean that during MIS 5, the population of the southern Cape followed a place provisioning strategy.

6. Conclusions

This study reports on the recently excavated KRM lithic material from layers SMONE and BOS from the SASL sub-member dating to between 100 and 110,000 years ago. Like previous studies on similarly aged material from KRM, the results indicate that a Levallois-like unidirectional reduction system was primarily used (Wurz, 2000, 2002). However, our analysis further details the various stages of this reduction sequence, not been described before. The semi-rotational platform cores and flat parallel cores, grouped into types I–V, have been shown to be most likely different parts of this reduction strategy. The in-depth study of the end products indicates that point shaped end products, including pointed flakes and blades dominate, a finding resonating with the previous analyses of broadly contemporaneous material from KRM (Wurz, 2000, 2002). Here it is also shown that three distinct types of points occur, also relating to different stages of reduction. A smaller blade component has been identified before (Wurz, 2000, 2002), and this analysis also confirms this. However, flakes as end products have not been previously described before, and it is shown here that whereas they are a consistent feature in the two assemblages studied, they are most frequent in SMONE. The correlation of core reduction sequences and end product morphology indicates a fluid system that aims for a combined manufacture of a variety of end product shapes. Another novel finding is the identification of a bladelet component in the assemblages, with bladelets especially frequent in SMONE. The formal tools, consisting of denticulates, notched tools and scrapers, occur in low frequencies, as at other MIS 5 MSA assemblages from South Africa.

Table 12
Core taxonomy for the KRM cores.

Core type (method)	Systematic reduction		Other	
	I	II–V	Bladelet cores	Tested, recycled, exhausted, altered, indeterminate, fragment
	Platform	Parallel		
Sub-type (morphology)	Pyramidal, prismatic, semi-rotational pyramidal, semi-rotational prismatic	Flat, natural lateral convexity (split cobble blanks)		
Orientation of production	Unidirectional (I)	Unidirectional (II–IV), bidirectional (V)	Unidirectional	Unidirectional, bidirectional multidirectional, indeterminate
Products	Blade, flake, point, bladelet	Flake, point	Bladelet	Flake, point, blade

They occur in addition to a more significant component of unretouched blanks with edge damage.

There are apparent differences between the SMONE and the BOS layers. This is especially seen in the different types of cores, and the frequency of different blank and end product types. Cores are more frequent in BOS, and core types II and V and bladelet cores only occur in BOS. More points and blades are present in BOS, whereas SMONE shows more focus on flakes and bladelets. Additionally, the blanks in BOS have more faceted platforms, and points are heavier than in SMONE. The formal tools are more frequent in BOS, as well as cores and hammerstones. This reflects differences in technological choices, and it may also reflect more ephemeral occupation in SMONE. This study shows the advantages of undertaking a detailed analysis of relatively small depositional units to investigate behavioral developments.

The material discussed here provides new information about the technological succession during MIS 5 at KRM. Moreover, it contributes to the understanding of the technology in the southern Cape region and

ultimately of Southern Africa. Although there exist local differences regarding reduction sequences and end product morphologies between the southern Cape sites, the similarities indicate common technological elements and place provisioning systems.

Acknowledgements

We want to thank the excavation team of Klasies River of the years 2015 and 2016, specifically Steven Walker and Silje Bentsen. We also acknowledge Joshua Kumbani for his help in the lab at the University of the Witwatersrand. Sarah Wurz and Mareike Brenner's research is supported by the National Research Foundation of South Africa, grant no 98826; any opinion, finding, conclusion or recommendation expressed in this article is that of the authors, and the NRF does not accept any liability in this regard. Three anonymous reviewers provided helpful comments that improved this paper.

Appendix A

Table A.1
Appearance of bulbs of proximally preserved debitage.

Bulb	SMONE		BOS	
	n	%	n	%
Well-defined	24	7.6%	70	11.2%
Defined	171	54.1%	383	61.5%
Removed	–	0%	2	0.3%
Poorly-defined	75	23.7%	130	20.9%
Absent	46	14.6%	38	6.1%
Total	316	100%	623	100%

Table A.2
Appearance of a ring crack of proximally preserved debitage.

Ring crack	SMONE		BOS	
	n	%	n	%
Circle	117	44.5%	522	87–1%
Half circle	90	34.2%	68	11.4%
None	56	21.3%	9	1.5%
Total	263	100%	599	100%

Table A.3
Maximal platform thickness average of proximally preserved debitage in mm.

Platform thickness average	SMONE		BOS	
	n	(mm)	n	(mm)
Blade (<i>n</i> = 239)	60	8.84	179	9.90
Bladelet (<i>n</i> = 18)	9	4.66	9	3.98
Point (<i>n</i> = 255)	52	8.21	203	11.79
Flake (<i>n</i> = 818)	309	10.77	509	9.65
Total	430	8.58	900	10.23

Table A.4
External platform angle average of proximally preserved debitage in °.

EPA average	SMONE		BOS	
	n	(°)	n	(°)
Blade	41	80.5°	122	87.5°
Bladelet	6	77.2°	3	75.0°
Point	40	78.3°	161	87.4°
Flake	216	85.6°	319	86.1°
Total	303	79.5°	605	87.1°

Table A.5
Appearance of lips of proximally preserved pieces.

Lip	SMONE		BOS	
	n	%	n	%
None	208	76.8%	531	89.7%
Traceable	53	19.6%	51	8.6%
Well defined	10	3.7%	10	1.7%
Total	271	100%	592	100%

Table A.6
Maximum dimension and weight of cores.

Core measurements	Number		Max. dimension (mm)	Weight (g)
	n			
SMONE	11		62.19	92.31
BOS	54		68.56	121.94
Total	65		67.40	116.55

Table A.7
Shapes of complete/almost complete flakes.

Flake shapes	SMONE		BOS	
	n	%	n	%
Flakes	131		191	
Rectangular	40		68	
Round/oval	23		36	
Expanding	18		35	
Sub-parallel	6		7	
Irregular	44		45	

Table A.8
Platform type of different blank types of proximally preserved blanks.

Platform type/blank type	Plain	Informal facet	Faceted	Cortical	Dihedral	Shattered	Total
SMONE	122	91	47	25	14	10	309
Point	5	17	12	4	1	2	41
Blade	6	20	12			2	40
Bladelet	4	1	1	1			7
Flake	107	53	22	20	13	6	221
BOS	202	155	174	41	23	18	615
Point	19	41	91	3	4	4	162

(continued on next page)

Table A.8 (continued)

Platform type/blank type	Plain	Informal facet	Faceted	Cortical	Dihedral	Shattered	Total
Blade	25	37	53	2	3	2	122
Bladelet	2			1		1	4
Flake	157	77	30	35	16	11	326
SMONE	39.5%	29.4%	15.2%	8.1%	4.5%	2.3%	100%
BOS	32.8%	25.2%	28.3%	6.7%	3.7%	2.9%	100%

Table A.9

Comparison between the KRM assemblages summarising the differences. Tests for normality was done for the continuous variable with a Shapiro-Wilk test (W). For normal distributions, the difference between the layers was tested with independent-samples *t*-tests (*t*). For data with non-normal distributions, Mann-Whitney *U* tests (*U*) were performed. An alpha level of .05 for all statistical tests is used. For *t*-tests and M-W tests, all *p*-values represent one-tailed tests. Chi-square tests (χ^2) were used for categorical data, with a degree of freedom of 1 (*d* = 1). (*significant).

Differences between assemblages	SMONE	BOS	S-W test for normality	<i>t</i> -Test or M-W and χ^2	statistical significance	
Assemblage composition	Amount of types	Less points (19.6%)		$\chi^2 = 7.16$, <i>p</i> .008*	Significantly different	
		Fewer blades (6.9%)		$\chi^2 = 3.90$, <i>p</i> .048*	Significantly different	
		More flakes (71.4%)	Less flakes (53.2%)		$\chi^2 = 4.31$, <i>p</i> .038*	Significantly different
		More bladelets (7.8%)	Less bladelets (3.3%)		$\chi^2 = 17.05$, <i>p</i> < .001*	Significantly different
		Less cores (1.8%)	More cores (4.3%)		$\chi^2 = 7.30$, <i>p</i> .007*	significantly different
Cores	Small debitage	77.2%	69.2%		$\chi^2 = 8.17$, <i>p</i> .004*	significantly different
	Core types	I, III, IV	I-V, bladelet cores			
	Core size	Smaller average max. dimension: 62.19 mm	Bigger average max. dimension: 68.56 mm	SMONE <i>W</i> = 0.96, <i>p</i> .846 BOS <i>W</i> = 0.97, <i>p</i> .164	<i>t</i> (66) = -1.34, <i>p</i> .092	Not significant
Tools		Lighter Average weight of 92.31 g	Heavier average weight 121.94 g	SMONE <i>W</i> = 0.66, <i>p</i> < .001* BOS <i>W</i> = 0.87, <i>p</i> < .001*	<i>U</i> = 221, <i>p</i> .058	Not significant
	Recycling of cores	No recycling (<i>n</i> = 0)	More recycling (<i>n</i> = 7)			
	Tool type frequency	Denticulate/notch (100%), Scraper (0%), Lateral retouch (0%)	Denticulate/notch (42.9%), Scraper (31.4%), Lateral retouch (25.7%)			
	Tool frequency	0.7% less frequent	2.8% more frequent		$\chi^2 = 8.91$, <i>p</i> .003*	Significantly different
	Edge damage frequency	16.4% less frequent	21.7% most frequent		$\chi^2 = 3.55$, <i>p</i> .059	not significant
End products	Hammerstone frequency	0.5% less frequent	2.0% more frequent		$\chi^2 = 6.17$, <i>p</i> .013*	significantly different
	EPA of points and blades	Narrow average EPA on points: 78.3°	Wider average EPA on points: 87.4°	SMONE <i>W</i> = 0.96, <i>p</i> .401 BOS <i>W</i> = 0.82, <i>p</i> < .001*	<i>U</i> = 1251.5, <i>p</i> .397	Significantly different
		Narrow average EPA on blades: 80.5°	Wider average EPA on blades: 87.5°	SMONE <i>W</i> = 0.93, <i>p</i> 0.164 BOS <i>W</i> = 0.88, <i>p</i> < .001*	<i>U</i> = 436, <i>p</i> .004*	Significantly different
	Platform type	Less faceting (35.3%)	More faceting (59.6%)		$\chi^2 = 4.21$, <i>p</i> .040*	Significantly different
	More informal faceting (45.6%)	Less informal faceting (25.0%)		$\chi^2 = 5.41$, <i>p</i> .020*	Significantly different	

(continued on next page)

Table A.9 (continued)

Differences between assemblages	SMONE	BOS	S-W test for normality	t-Test or M-W and χ^2	statistical significance
Proximal preparation	Fewer dihedral platforms (1.5%)	Some dihedral platforms (2.5%)		$\chi^2 = 0.24$, $p = 0.622$	Not significant
	Some rubbing (4.3%)	Less rubbing (0.2%)		$\chi^2 = 1.62$, $p = .203$	Not significant
	Less invasive preparation (longer removals along scar ridges) (42%)	More invasive preparation (longer removals along scar ridges) (51.4%)		$\chi^2 = 0.51$, $p = .476$	Not significant
	Platform thickness (average mm)	Thinner platform on points: 8.2 mm	Thicker platform on points: 11.8 mm	SMONE $W = 0.97$, $p = .743$ BOS $W = 0.89$, $p = .099$	$t(138) = -1.10$, $p = .137$
Platform thickness (average mm)	Thinner platform on blades: 8.8 mm	Thicker platform on blades: 9.9 mm	SMONE $W = 0.90$, $p = .429$ BOS $W = 0.96$, $p = .516$	$t(98) = 1.32$, $p = .096$	Not significant
	Thicker platform on flakes: 10.8 mm	Thinner platform on flakes: 9.7 mm	SMONE $W = 0.97$, $p = .550$ BOS $W = 0.94$, $p = 0.034^*$	$U = 433$, $p = .087$	Not significant
	Weight	Points are lighter (average weight 21.7 g)	Points are heavier (average weight 29.7 g)	SMONE $W = 0.93$, $p = .164$ BOS $W = 0.86$, $p < .001^*$	$U = 733$, $p = .038^*$
Blades are lighter (average weight 24 g)		Blades are heavier (average weight 30.4 g)	SMONE $W = 0.84$, $p = .116$ BOS $W = 0.93$, $p = .124$	$t(28) = -0.97$, $p = .171$	Not significant
Flakes are lighter (average weight 17.8 g)		Flakes are heavier (average weight 37.3 g)	SMONE $W = 0.95$, $p = .685$ BOS $W = 0.88$, $p = .0285584^*$	$U = 69$, $p = .074$	Not significant
Dimensions	Points are narrower (32.7 mm)	Points are wider (36.8 mm)	SMONE $W = 0.94$, $p = .296$ BOS $W = 0.91$, $p < .001^*$	$U = 687$, $p = .034^*$	Significantly different
	Points are thinner (12.1 mm)	Points are thicker (13.3 mm)	SMONE $W = 0.97$, $p = .729$ BOS $W = 0.97$, $p = .045^*$	$U = 764$, $p = .061$	Not significant
	Blades are narrower (27.5 mm)	Blades are wider (29.8 mm)	SMONE $W = 0.91$, $p = .403$ BOS $W = 0.98$, $p = .884$	$t(28) = -0.74$, $p = .232$	Not significant
	Blades are thinner (11.6)	Blades are thicker (12.4 mm)	SMONE $W = 0.90$, $p = .343898$ BOS $W = 0.97$, $p = .749$	$t(28) = -0.83$, $p = .208$	Not significant
	Flakes are narrower (33.8 mm)	Flakes are wider (39.2 mm)	SMONE $W = 0.97$, $p = .879$ BOS $W = 0.96$, $p = .702$	$t(28) = -1.32$, $p = .099$	Not significant
Dorsal scar patterning	Flakes are thinner (11.2 mm)	Flakes are thicker (13.9 mm)	SMONE $W = 0.96$, $p = .851$ BOS $W = 0.96$, $p = .551$	$t(28) = -1.70$, $p = .050$	Not significant
	Mostly unidirectional (63.9%)	Mostly unidirectional (54.1%)		$\chi^2 = 0.30$, $p = .585$	Not significant
	Less bidirectional (16.7%)	More bidirectional (23.3%)		$\chi^2 = 0.48$, $p = .487$	Not significant

Table A.10
Comparative table of MIS 5 assemblages from the southern Cape. The abbreviation ni stands for no information.* (% of complete blanks).

Site	Assemblage	MIS	Dating	Raw materials	% triangular flakes*	% blade sized points*	% blades*	% flakes*	% bladelets (of all debitage > 20 mm)	% faceted platforms (of pieces with pre-served platforms)	% tools (of all debitage > 20 mm)	% edge damage (of all debitage > 20 mm)	Tool types	Source
Klasiess River	SMONE	MIS 5c-d		100% local: quartzite (92%), quartz (7%), sandstone, silcrete (< 1%)	9.6%	8.6%	6.9%	71.4%	7.8% (including < 20 mm)	15.2%	0.7%	16.4%	Denticulate, notch	this paper
BOS		MIS 5c-d		100% local: quartzite (84.9%), quartz (15%), sandstone (1%)	16.8%	7.5%	12.9%	53.2%	3.3% (including < 20 mm)	28.3%	2.8%	21.7%	Denticulate, notch, scraper, lateral retouch	
Pinnacle Point 13B	SBS/URS (East)	MIS 5c	94 ± 3 ka OSL	> 90% local: quartzite (84.9%), quartz (11.5%), silcrete (2.7%)	7.2% (flake- and blade-sized points of complete and broken blanks and chunks)	11.5% (of complete and broken blanks and chunks)	11.5% (of complete and broken blanks and chunks)	55.9% (of complete and broken blanks and chunks)	0.5%	27.5%	2.1% incl. < 20 mm	< 20 mm	Bulbar thinning, notch, backed, denticulate, burin-like retouch	Thompson et al. (2010), Jacobs (2010)
	LBS1 and UDBS Unit (West)	MIS 5c	99 ± 4 ka, 124 ± 5 ka OSL	> 90% local: quartzite (80.8%), quartz (13.3%), < 10% non-local: silcrete (3.9%)	12.7% (flake- and blade-sized points of complete and broken blanks and chunks)	9.8% (of complete and broken blanks and chunks)	9.8% (of complete and broken blanks and chunks)	49% (of complete and broken blanks and chunks)	0.8%	23.7%	4% incl. < 20 mm	< 20 mm	Bulbar thinning, notch, backing, denticulate, burin-like retouch	
	Lower Roof Spall	MIS 5d	110 ± 4 ka OSL	> 90% local: quartzite (88.1%), quartz (9.5%), < 10% non-local: silcrete (2.4%)	2.4% (flake- and blade-sized points of complete and broken blanks and chunks)	4.7% (of complete and broken blanks and chunks)	4.7% (of complete and broken blanks and chunks)	54.8% (of complete and broken blanks and chunks)	0%	28%	0% incl. < 20 mm	< 20 mm	–	
	LC-MSA Upper/Middle	MIS 5e	125 ± 5 ka OSL	85.7% local: quartzite (77.9%), quartz (7.8%), 12.6% non-local: silcrete	8.7% (flake- and blade-sized points of complete and broken blanks and chunks)	13% (of complete and broken blanks and chunks)	13% (of complete and broken blanks and chunks)	57.6% (of complete and broken blanks and chunks)	0.9%	26.3%	1.7% incl. < 20 mm	< 20 mm	Bulbar thinning, notch, backing, denticulate, burin-like retouch	
Pinnacle Point 5–6	LBSLR Jed/JR Quartzite	MIS 5a-b	86 ± 3 ka - 79 ± 3 ka OSL	Quartzite (95%), silcrete, chert, homfels, quartz	63% (points of end products)	37% (of end products)	37% (of end products)	ni	ni	33% (of complete blanks)	0%	3.8% incl. < 20 mm	–	Brown (2011)
Cape St Blaize	C1–4 and CU	MIS 5	–	100% local: quartzite (92%), silcrete, calcedony, hornfels, shale, quartz	7.7% (probably including fragments)	ni	22.8% (probably including fragments)	52.6% (probably including fragments)	ni	51.9%	12.8% (Goodwin: 5.8%)	ni	“General retouch”, notch, denticulate, backing	Thompson and Marean (2008), Goodwin (2008), Goodwin and Malan (1935)
Blombos	M3 phase	MIS 5c-b	101 ± 4 ka - 94 ± 3 ka OSL, U/Th	100% local: silcrete (65%), quartzite (19%), quartz (17%), other (1%)	20%	No differentiation to blades	8%	72%	0%	15.7%	2.3%	1.3%	notch, denticulate, scraper, short retouch, borer, burin	Douze et al. (2015)

References

- Andrefsky, W., 2005. *Lithics: Macroscopic Approaches to Analysis* (Cambridge Manuals in Archaeology). Cambridge University Press Cambridge.
- Avery, G., Cruz-Uribe, K., Goldberg, P., Grine, F.E., Klein, R.G., Lenardi, M.J., Marean, C.W., Rink, W.J., Schwarcz, H.P., Thackeray, A.I., 1997. The 1992–1993 excavations at the Die Kelders Middle and Later Stone Age cave site, South Africa. *J. Field Archaeol.* 24, 263–291.
- Avery, G., Halkett, D., Orton, J., Steele, T., Tusenius, M., Klein, R., 2008. The Ysterfontein 1 Middle Stone Age rock shelter and the evolution of coastal foraging. In: *Goodwin Series*, pp. 66–89.
- Backwell, L.R., d'Errico, F., Banks, W.E., de la Peña, P., Sievers, C., Stratford, D., Lennox, S.J., Wojcieszak, M., Bordy, E.M., Bradfield, J., 2018. New excavations at Border Cave, Kwa Zulu-Natal, South Africa. *J. Field Archaeol.* 1–20.
- Bar-Yosef, O., Van Peer, P., 2009. The chaîne opératoire approach in Middle Paleolithic archaeology. *Curr. Anthropol.* 50, 103–131.
- Bentsen, S., Wurz, S., 2017. Towards a better understanding of cooking techniques in the African Middle Stone Age. *Primit. Tider.* 19, 101–115.
- Bentsen, S.E., Wurz, S., 2019. Color me heated? A comparison of potential methods to quantify color change in thermally altered rocks. *J. Field Archaeol.* 44 (4), 215–233.
- Binford, L., 1977. Forty-seven Trips: A Case Study in the Character of Archaeological Formation Processes. *Stone Tools as Cultural Markers: Change, Evolution and Complexity*. pp. 24–36.
- Breizillon, M., 1968. La dénomination des objets de Pierre taillée. *Materiaux pour un vocabulaire des préhistoriens de langue française IV supplément a "Galla préhistoire."* P. CNRS.
- Brown, K.S., 2011. The Sword in the Stone: Lithic raw material in the Middle Stone Age at Pinnacle Point Site 5–6. (southern Cape, South Africa).
- Carr, A.S., Chase, B.M., Mackay, A., 2016. Mid to Late Quaternary landscape and environmental dynamics in the Middle Stone Age of southern South Africa. In: *Africa from MIS 6–2*. Springer, pp. 23–47.
- Compton, J.S., 2011. Pleistocene sea-level fluctuations and human evolution on the southern coastal plain of South Africa. *Quat. Sci. Rev.* 30, 506–527.
- Conard, N.J., 2012. *Klingentechnologie vor dem Jungpaläolithikum*. Tübingen Publications in Prehistory. Steinartefakte. Vom Altpaläolithikum bis in die Neuzeit. pp. 245–266.
- Conard, N.J., Soressi, M., Parkington, J.E., Wurz, S., Yates, R., 2004. A unified lithic taxonomy based on patterns of core reduction. *South African Archaeological Bulletin* 59, 12–16.
- Cowling, R., 1984. Syntaxonomic and synecological study in the Humansdorp region of the Fynbos Biome. (Bothalia).
- Crabtree, D.E., 1972. The cone fracture principle and the manufacture of lithic materials. *Tebiwa* 15, 29–42.
- Damlien, H., 2015. Striking a difference? The effect of knapping techniques on blade attributes. *J. Archaeol. Sci.* 63, 122–135.
- Deacon, J., 1984. The Later Stone Age of Southernmost Africa. *BAR*.
- Deacon, H.J., 1995. Two late Pleistocene-Holocene archaeological depositories from the southern cape, South Africa. *The South African Archaeological Bulletin* 121–131.
- Deacon, H.J., 2008. The context of the 1967-8 sample of human remains from Cave 1 Klasies River main site. In: *Goodwin Series*, pp. 143–149.
- Deacon, H.J., Geleijnse, V.B., 1988. The stratigraphy and sedimentology of the main site sequence, Klasies River, South Africa. In: *The South African Archaeological Bulletin*, pp. 5–14.
- Dibble, H.L., Rezek, Z., 2009. Introducing a new experimental design for controlled studies of flake formation: results for exterior platform angle, platform depth, angle of blow, velocity, and force. *J. Archaeol. Sci.* 36, 1945–1954.
- Dibble, H.L., Holdaway, S.J., Lin, S.C., Braun, D.R., Douglass, M.J., Iovita, R., McPherron, S.P., Olszewski, D.I., Sandgathe, D., 2017. Major fallacies surrounding stone artifacts and assemblages. *J. Archaeol. Method Theory* 24, 813–851.
- Douze, K., Wurz, S., Henshilwood, C.S., 2015. Techno-Cultural Characterization of the MIS 5 (c. 105–90 Ka) Lithic Industries at Blombos Cave, Southern Cape, South Africa. *PLoS one* e0142151.
- Dusseldorp, G., Lombard, M., Wurz, S., 2013. Pleistocene Homo and the updated Stone Age sequence of South Africa. *S. Afr. J. Sci.* 109, 01–07.
- Eggs, S.M., Grün, R., McCulloch, M.T., Pike, A.W.G., Chappell, J., Kinsley, L., Mortimer, G., Shelley, M., Murray-Wallace, C.V., Spötl, C., Taylor, L., 2005. In situ U-series dating by laser-ablation multi-collector ICPMS: new prospects for Quaternary geochronology. *Quat. Sci. Rev.* 24, 2523–2538.
- Feathers, J.K., 2002. Luminescence dating in less than ideal conditions: case studies from Klasies River main site and Duinefontein, South Africa. *J. Archaeol. Sci.* 29, 177–194.
- Geneste, J.-M., 1985. *Analyse lithique d'industries moustériennes du Périgord: une approche technologique du comportement des groupes humains au Paléolithique moyen*. University of Bordeaux I.
- Goodwin, A., 1930. Chronology of the Mossel Bay industry. *S. Afr. J. Sci.* 27, 562–572.
- Goodwin, A.J.H., Malan, B.D., 1935. Archaeology of the Cape St. Blaize cave and raised beach, Mossel Bay. *Annals of the South African Museum* XXIV, 111–140.
- Goodwin, A., van Riet Lowe, C., 1929. The Stone Age cultures of South Africa, Cape Town. *Annals of the South African Museum*, pp. 27.
- Grine, F.E., Wurz, S., Marean, C.W., 2017. The middle stone age human fossil record from Klasies River main site. *J. Hum. Evol.* 103, 53–78.
- de Heinzelin de Braucourt, J., 1962. *Manuel de typologie des industries lithiques*. Commission Administrative du Patrimoine de l'Institut Royal des Sciences Naturelles de Belgique.
- Jacobs, Z., 2010. An OSL chronology for the sedimentary deposits from Pinnacle Point Cave 13B—A punctuated presence. *J. Hum. Evol.* 59, 289–305.
- Kuhn, S.L., 1992. On planning and curated technologies in the Middle Paleolithic. *J. Anthropol. Res.* 48, 185–214.
- Kuhn, S.L., 1995. *Mousterian Lithic Technology and raw material economy*. Princeton University Press.
- Kuman, K., Inbar, M., Clarke, R.J., 1999. Palaeoenvironments and cultural sequence of the Florisbad Middle Stone Age hominid site, South Africa. *J. Archaeol. Sci.* 26, 1409–1425.
- Mackay, A., 2016. Technological change and the importance of variability: The Western Cape of South Africa from MIS 6-2. In: *frica from MIS 6-2*. Springer, pp. 49–63.
- Mackay, A., Stewart, B.A., Chase, B.M., 2014. Coalescence and fragmentation in the late Pleistocene archaeology of southernmost Africa. *J. Hum. Evol.* 72, 26–51.
- Mackay, A., Jacobs, Z., Steele, T.E., 2015. Pleistocene archaeology and chronology of Putslaagte 8 (PL8) rockshelter, Western Cape, South Africa. *Journal of African Archaeology* 13, 71–98.
- Mackay, A., Hallinan, E., Steele, T.E., 2018. Provisioning responses to environmental change in South Africa's winter rainfall zone: MIS 5-2. In: *Lithic Technological Organization and Paleoenvironmental Change*. Springer, pp. 13–36.
- Marean, C.W., Nilssen, P.J., Brown, K., Jerardino, A., Stuyder, D., 2004. Paleoanthropological investigations of Middle Stone Age sites at Pinnacle Point, Mossel Bay (South Africa): archaeology and hominid remains from the 2000 field season. *Paleoanthropology* 2.
- Millard, A.R., 2008. A critique of the chronometric evidence for hominid fossils: I. Africa and the Near East 500–50 ka. *J. Hum. Evol.* 54, 848–874.
- Pelcin, A.W., 1997. The formation of flakes: the role of platform thickness and exterior platform angle in the production of flake initiations and terminations. *J. Archaeol. Sci.* 24, 1107–1113.
- Porraz, G., Parkington, J.E., Rigaud, J.-P., Miller, C.E., Poggenpoel, C., Tribolo, C., Archer, W., Cartwright, C.R., Charrié-Duhaut, A., Dayet, L., 2013a. The MSA sequence of Diepkloof and the history of southern African Late Pleistocene populations. *J. Archaeol. Sci.* 40, 3542–3552.
- Porraz, G., Texier, P.-J., Archer, W., Piboule, M., Rigaud, J.-P., Tribolo, C., 2013b. Technological successions in the Middle Stone Age sequence of Diepkloof Rock Shelter, Western Cape, South Africa. *J. Archaeol. Sci.* 40, 3376–3400.
- Porraz, G., Val, A., Tribolo, C., Mercier, N., de la Peña, P., Haaland, M.M., Igreja, M., Miller, C.E., Schmid, V.C., 2018. The MIS5 Pietersburg at '28' Bushman Rock Shelter, Limpopo Province, South Africa. *PLoS One* 13, e0202853.
- Rots, V., Lentfer, C., Schmid, V.C., Porraz, G., Conard, N.J., 2017. Pressure flaking to serrate bifacial points for the hunt during the MIS5 at Sibudu Cave (South Africa). *PLoS One* 12, e0175151.
- Schmid, V.C., Conard, N.J., Parkington, J.E., Texier, P.-J., Porraz, G., 2016. The 'MSA 1' of Elands Bay Cave (South Africa) in the context of the southern African Early MSA technologies. *South. Afr. Humanit.* 29, 153–201.
- Shimelmitz, R., Kuhn, S.L., 2018. The toolkit in the core: there is more to Levallois production than predetermination. *Quat. Int.* 464, 81–91.
- Shott, M., Tostevin, G., 2015. Diversity under the bipolar umbrella. *Lithic Technol.* 40, 377–384.
- Singer, R., Wymer, J., 1982. *The Middle Stone Age at Klasies River Mouth in South Africa*. University of Chicago Press.
- de Sonneville-Bordes, D. de, 1960. *Le Paléolithique supérieur en Périgord*. Delmas, Bordeaux.
- de Sonneville-Bordes, D., Perrot, J., 1954. *Lexique typologique du Paléolithique supérieur: Outillage lithique: I Grattoirs-II Outils solutréens*. *Bulletin de la Société préhistorique de France* 51, 327–335.
- Soriano, S., Villa, P., Wadley, L., 2007. Blade technology and tool forms in the Middle Stone Age of South Africa: the Howiesons Poort and post-Howiesons Poort at Rose Cottage Cave. *J. Archaeol. Sci.* 34, 681–703.
- Soriano, S., Villa, P., Delagnes, A., Degano, I., Pollarolo, L., Lucejko, J.J., Henshilwood, C., Wadley, L., 2015. The Still Bay and Howiesons Poort at Sibudu and Blombos: understanding Middle Stone Age technologies. *PLoS One* 10, e0131127.
- Speth, J.D., 1981. The role of platform angle and core size in hard-hammer percussion flaking. *Lithic Technol.* 10, 16–21.
- Thackeray, A.I., 1989. Changing fashions in the Middle Stone Age: the stone artefact sequence from Klasies River main site, South Africa. *Afr. Archaeol. Rev.* 7, 33–57.
- Thackeray, A.I., Kelly, A.J., 1988. A technological and typological analysis of Middle Stone Age assemblages antecedent to the Howiesons Poort at Klasies River main site. *The South African Archaeological Bulletin* 15–26.
- Thompson, E., Marean, C.W., 2008. The Mossel Bay lithic variant: 120 Years of Middle Stone Age research from Cape St Blaize Cave to Pinnacle Point. *Goodwin Series*, vol. 10.
- Thompson, E., Williams, H.M., Minichillo, T., 2010. Middle and late Pleistocene Middle Stone Age lithic technology from Pinnacle Point 13B (Mossel Bay, Western Cape province, South Africa). *J. Hum. Evol.* 59, 358–377.
- Tixier, J., 1963. *Typologie de l'Épipaléolithique du Maghreb*. *Mémoires du centre de recherches anthropologiques, préhistoriques et ethnographiques*. Arts et Métiers Graphiques, Paris.
- Tribolo, C., Mercier, N., Selo, M., Valladas, H., Joron, J., Reyss, J., Henshilwood, C., Sealy, J., Yates, R., 2006. TL dating of burnt lithics from Blombos Cave (South Africa): further evidence for the antiquity of modern human behaviour. *Archaeometry* 48, 341–357.
- Van Andel, T.H., 1989. Late Quaternary sea-level changes and archaeology. *Antiquity* 63, 733–745.
- Villa, P., Delagnes, A., Wadley, L., 2005. A late Middle Stone Age artifact assemblage from Sibudu (KwaZulu-Natal): comparisons with the European Middle Paleolithic. *J. Archaeol. Sci.* 32, 399–422.
- Vogel, J.C., 2001. Radiometric dates for the Middle Stone Age in South Africa. In: *Humanity from African Naissance to Coming Millennia*, pp. 1000–1008.

- Volman, T.P., 1978. Early archeological evidence for shellfish collecting. *Science* 201, 911–913.
- Volman, T.P., 1981. *The Middle Stone Age in the Southern Cape* (PhD Thesis). University of Chicago, Department of Anthropology.
- Wadley, L., 2015. Those marvellous millennia: the Middle Stone Age of southern Africa. *Azania: Archaeological Research in Africa* 50, 155–226.
- Wang, Q., Tobias, P., Roberts, D., Jacobs, Z., 2008. A re-examination of a human femur found at the Blind River site, East London, South Africa: its age, morphology, and breakage pattern. *Anthropol. Rev.* 71, 43–61.
- van Wijk, Y., Tusenius, M.L., Rust, R., Cowling, R.M., Wurz, S., 2017. Modern vegetation at the Klasies River archaeological sites, Tsitsikamma coast, south-eastern Cape, South Africa: a reference collection. *Plant Ecology and Evolution* 150, 13–34.
- Will, M., Parkington, J.E., Kandel, A.W., Conard, N.J., 2013. Coastal adaptations and the Middle Stone Age lithic assemblages from Hoedjiespunt 1 in the Western Cape, South Africa. *J. Hum. Evol.* 64, 518–537.
- Wurz, S., 2000. *The Middle Stone Age at Klasies River, South Africa* (PhD Thesis). Stellenbosch University, Stellenbosch.
- Wurz, S., 2002. Variability in the Middle Stone Age lithic sequence, 115,000–60,000 years ago at Klasies River, South Africa. *J. Archaeol. Sci.* 29, 1001–1015.
- Wurz, S., 2012. The significance of MIS 5 shell middens on the Cape coast: a lithic perspective from Klasies River and Ysterfontein 1. *Quat. Int.* 270, 61–69.
- Wurz, S., 2013. Technological trends in the Middle Stone Age of South Africa between MIS 7 and MIS 3. *Curr. Anthropol.* 54, 305–319.
- Wurz, S., Bentsen, S.E., Reynard, J., Van Pletzen-Vos, L., Brenner, M., Mentzer, S., Pickering, R., Green, H., 2018. Connections, culture and environments around 100 000 years ago at Klasies River main site. *Quat. Int.* 495, 102–115.